ADDIS ABABA UNIVERSITY

GRADUATE STUDIES PROGRAM

SCHOOL OF EARTH SCIENCES

STRUCTURES AND KINEMATICS OF THE EASTERN MARGIN OF CENTRAL MAIN ETHIOPIAN RIFT

BY: YEWUBDAR DOGISSO

A Thesis submitted to the School of Graduate Studies, Addis Ababa University, in partial fulfillment of the requirements of the Degree of Masters of Science in Structural Geology

June, 2016

This is to certify that thesis prepared by YEWUBDAR DOGISSO GONA, entitled: "**Structures and kinematics of the eastern margin of Central Main Ethiopian rift"** and submitted in partial fulfillment of the requirements for the Degree of Master of Science in Structural Geology compiles with the regulations of the University and meets the accepted standards with respect to the originality and quality.

SIGNED BY THE EXAMINING COMMITTEE:

EXAMINER

Dr. Bekele Abebe Signature _____ Date _____

Dr. Mulugeta Alene Signature _____ Date _____

ADVISOR

Dr. Ameha Atnafu Signature _____ Date _____

CHAIRPERSON OF DEPARTMENT

Dr. Balmwal Atnafu Signature _____ Date _____

ABSTRACT

This study presents the kinematics and the tectonics of the eastern margin of central Main Ethiopian rift based on detail structural field investigation. Field mapping and structural analysis from thirteen at high angle (~ 60°) normal fault blocks across the eastern margin with a total of 28 fault slip data are collected and analyzed. All kinematic indicators show a dip slip movement with rake values close to 90°. The kinematic analysis yields a minimum horizontal compressive stress oriented in N120°E. This extension direction is almost similar to independent structural analysis and earthquake focal mechanism inversions. This hints that the central MER is characterized by a constant extensional tectonics during at least Quaternary.

ACKNOWLEDGEMENT

I deeply acknowledge my advisor; Dr. Ameha Atnafu for his closeness and constructive advises and comments he gave for the progress and success of this study.

Immeasurable thanks goes to Solomon G\Michael, who have contributed a lot to the completion of this work.

Finally, above all I would like to thank to God for being with me all the time in my life and setting ways to the success of this work.

LIST OF CONTENTS

CONTENTS

LIST OF TABLES

LIST OF FIGURES

ACRONYM

BRZ: Broadly Rifted Zone

CER: Central Ethiopian Rift

CMER: Central Main Ethiopian Rift

EARS: East African Rift System

MER: Main Ethiopian Rift

NMER: Northern Main Ethiopian Rift

SDFZ: Silti Debre Zeit Fault Zone

SMER: Southern Main Ethiopian Rift

WFB: Wonji Fault Belt

CHAPTER ONE

1. INTRODUCTION

1.1 BACKGROUND

The Main Ethiopian Rift is a roughly NE trending sector of the East African Rift system that includes series of rift segments extending from the Afar Triple Junction at the Red Sea-Gulf of Aden intersection to the Kenya Rift (Bonini et al., 2005). The Main Ethiopian Rift is a region of rifting that accommodates the active separation between the Nubia and Somalia Plates (e.g. Corti, 2009). The Main Ethiopian Rift (in Fig 1.1) is characterized by active extensional tectonics accommodating the ~6–7 mm/yr relative movement between the African and Somalian plates [e.g., Chu and Gordon, 1999; Fernandes et al., 2004].

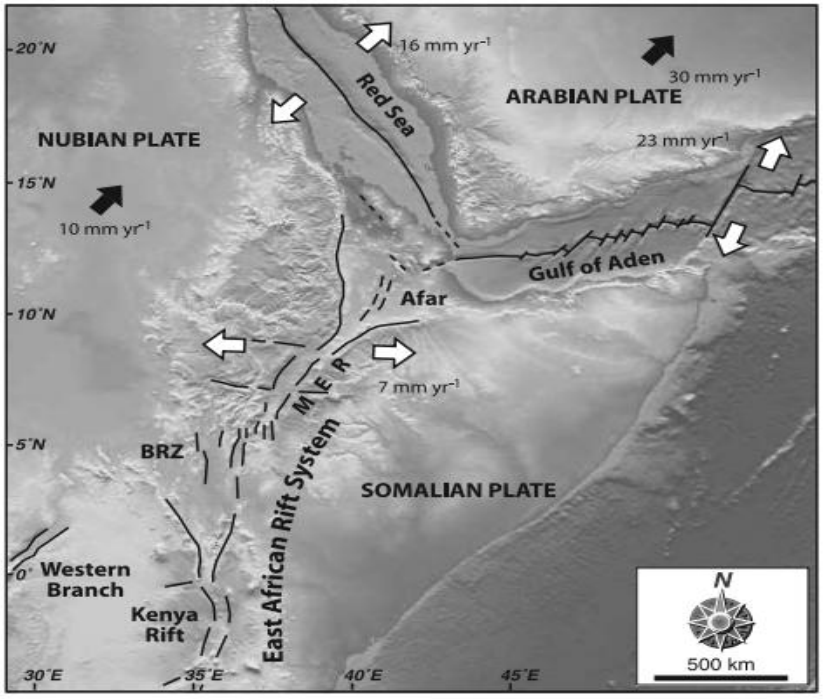

Fig. 1.1 Tectonic setting of the Main Ethiopian Rift (MER). White arrows indicate the direction and magnitude of extension in the MER of relative plate velocities; Red Sea [Le Pichon and Gaulier, 1988]; Gulf of Aden [Jestin et al., 1994]; Main Ethiopian Rift [Fernandes et al., 2004]. Black arrows indicate absolute plate motion direction and magnitude [Argus and Gordon, 1991]. BRZ the broadly rifted zone of southern Ethiopia.

Active faulting and volcanic activity is mostly localized along N-S to N20^0 trending fault system (Wonji Fault Belt) developed with in the rift floor [e.g., Mohr, 1962, 1987; Gibson, 1969; Mohr and Wood, 1976; Kazmin, 1980]. The Main Ethiopian Rift is traditionally differentiated into three main sectors differing in terms of rift trend, fault patterns and lithospheric characteristics: Northern MER (NMER), Central MER (CMER), and Southern MER (SMER) (e.g. Bonini et al., 2005; [Hayward and Ebinger, 1996;] Mohr, 1983). Below (Fig 1.2) shows this three main Ethiopian different sectors.

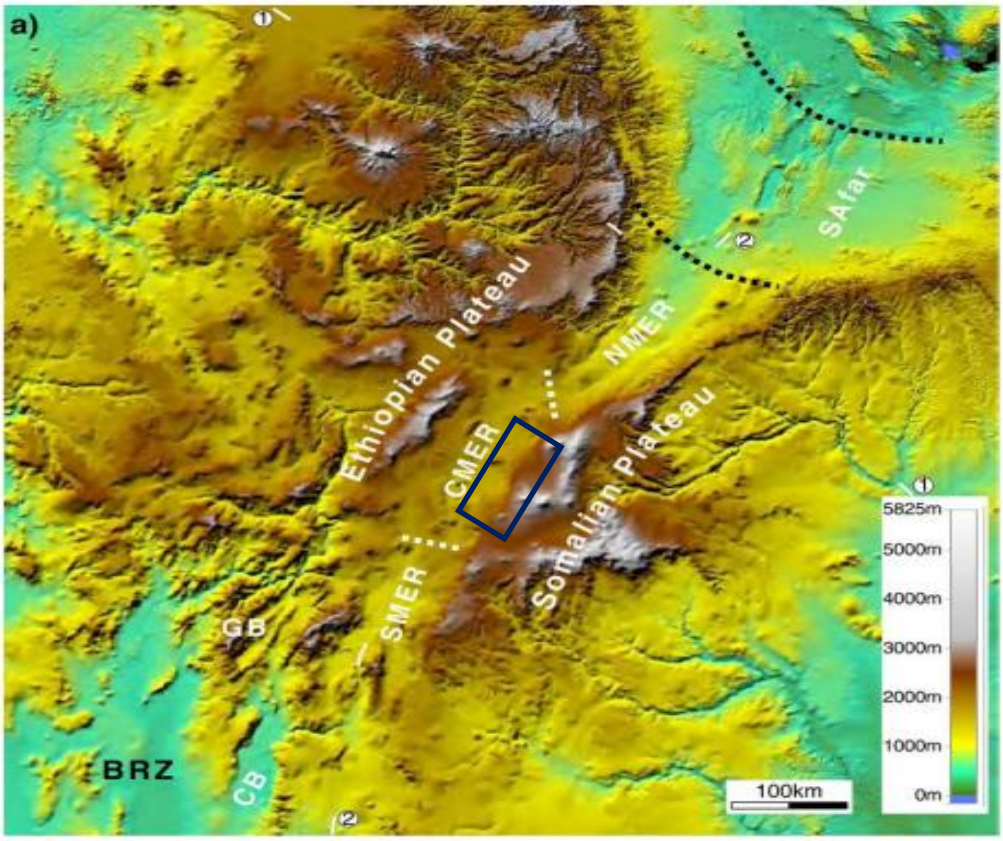

Fig. 1.2 Digital elevation model of the Ethiopian Rift showing the three main rift segments: (from north to south) Southern Afar, Northern Main Ethiopian Rift (NMER), Central Main Ethiopian Rift (CMER) and Southern Main Ethiopian Rift (SMER). BRZ: Broadly Rifted Zone; CB: Chow Bahir Rift; GB: Gofa Basin and Range. (Corti, 2009). The rectangle represents for CMER where the present study is takes place on its eastern margin.

The different Main Ethiopian Rift sectors are characterized by two distinct systems of normal faults that differ in terms of orientation, structural characteristics timing of activation and relation with magmatism: these are border faults and a set of faults affecting the rift floor referred as Tectono-magmatic segments (e.g., Boccaletti et al., 1998; Mohr, 1962).

The Central Main Ethiopian Rift encompasses most of the Lakes Region; lake Ziway, lake Abiyata, lake Langano, lake Shala up to the Lake Awasa area. The morpho-tectonic structure of the Lake Langano is controlled by a general NNE fault trend which is directly related to the evolution of the Gadamsa–East Ziway and Ziway–Shala Wonji Fault Belt (Le Turdu 1999).

1.2 TOPOGRAPHY

The Ethiopian Rift valley extends from the Kenyan border up to the Red Sea and divides the Ethiopian highlands into a northern and southern halve. The floor of the Rift valley encompasses three major water basins from NE to SW: Topographic features of main Ethiopian rift is given in Fig 1.3.

- Awash basin with the Koka, Beseka, Gemari, and Abe as most important lakes.
- Central Ethiopian Rift (CER) valley with the Ziway, Langano, Abyata and Shala lakes as most important lakes.
- Southern basin with Awassa, Abaya, Chamo and Chew-Bahir as most important lakes.

These three basins may be connected by underground faults running in NE – SW direction (Ayenew, 2004).

The Lake Region of Ethiopia lies in the central sector of the Main Ethiopian Rift is part of the northern branch of the East Africa Rift system. The four major lakes are; Ziway, Langano, Abiyata and Shala. The drainage and topography of the four lakes is shown in Fig 1.4.

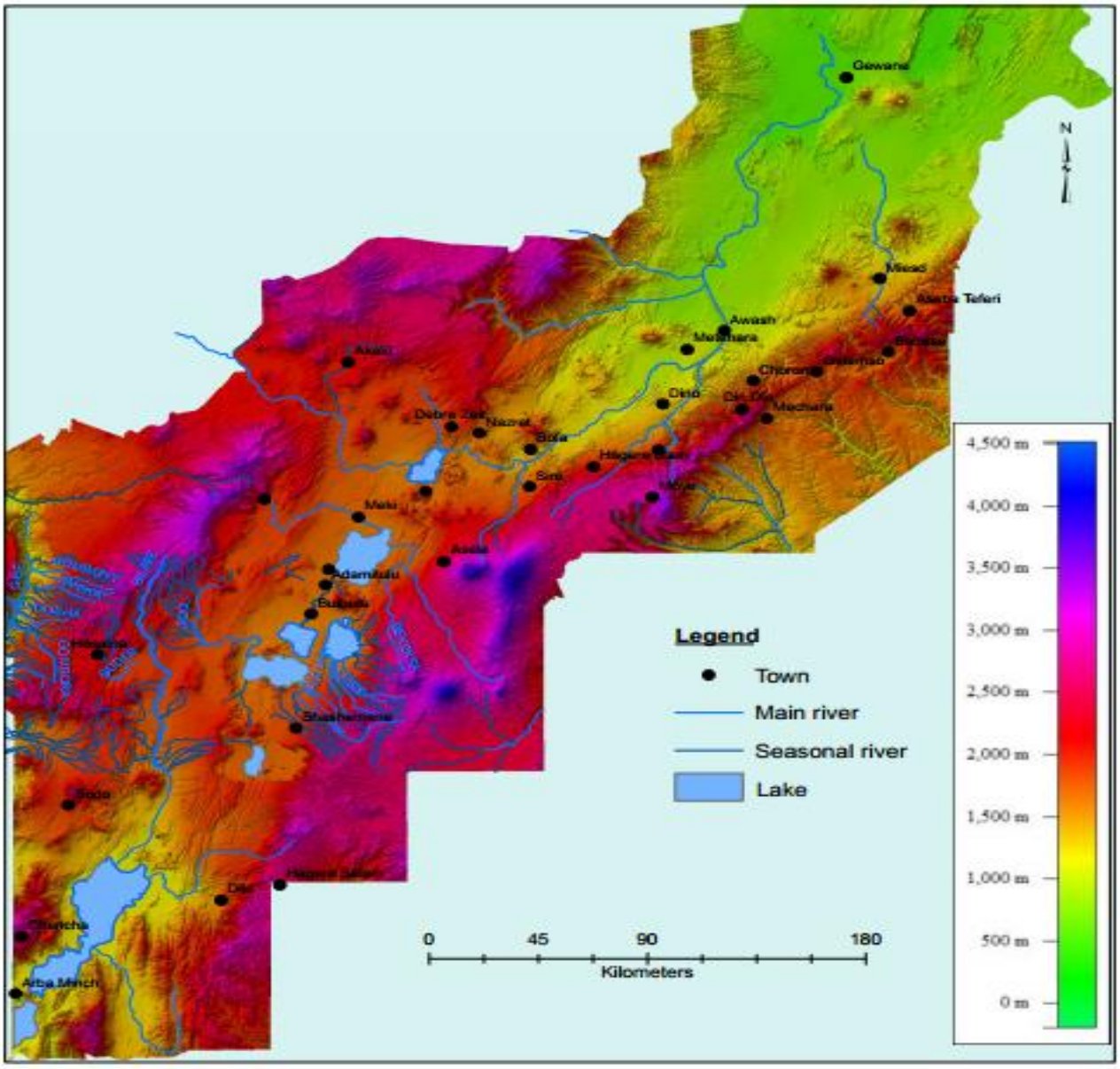

Fig. 1.3 Topographic map of Main Ethiopian rift

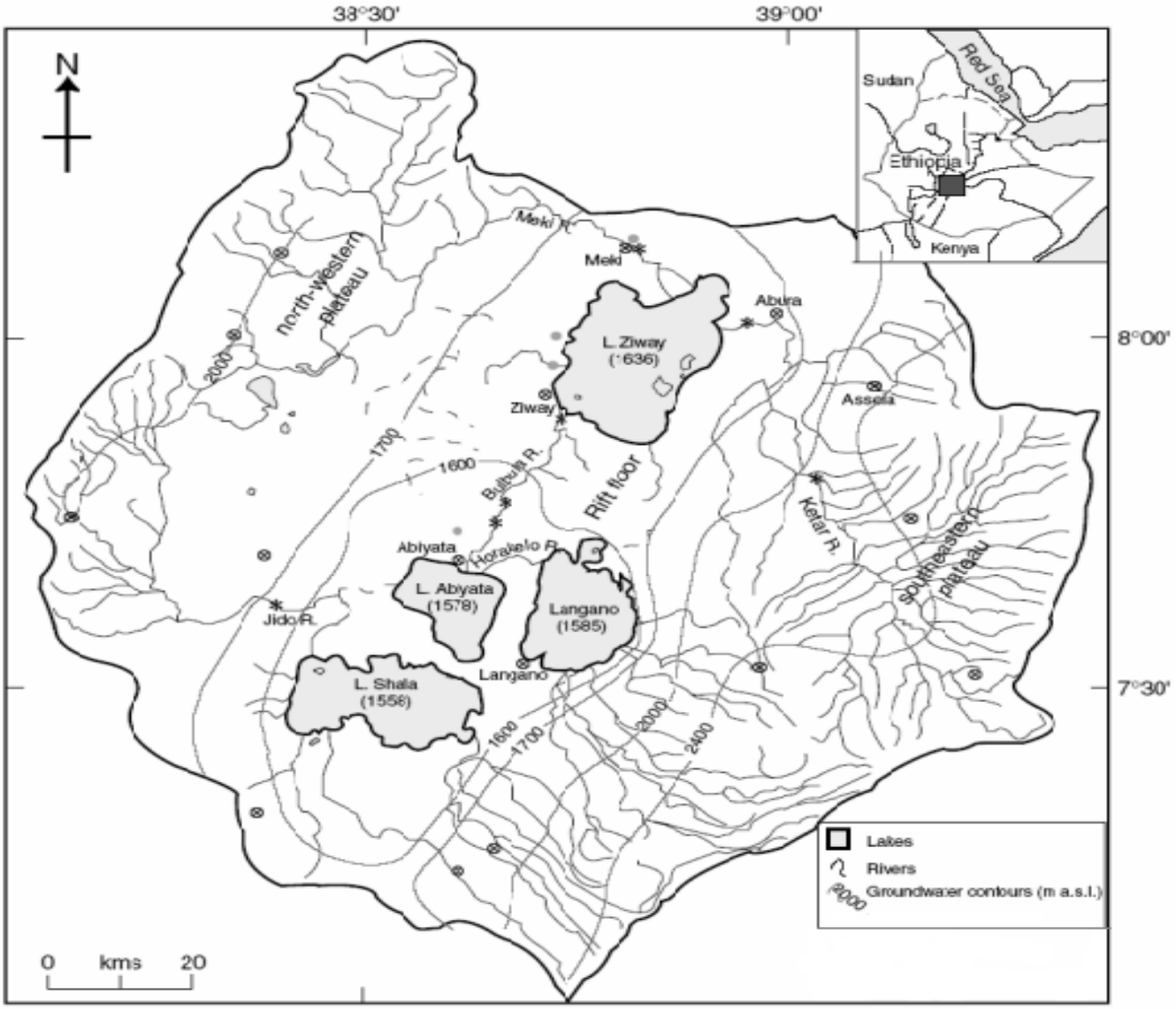

Fig. 1.4 Topography and drainage pattern of the Central Main Ethiopian Rift (Legesse et al., 2004)

1.3 LOCATION OF THE STUDY AREA

The study area is located at the eastern margin of central main Ethiopian rift. The area stretches from eastern part of Lake Langano, Lake Ziway up to Asela. Langano is a lake in the Oromia Region of Ethiopia, found at 200 Kms by road south of the capital, Addis Ababa, on border between the east Shewa and Arsi Zones. It has surface area of 230 Km^2 and surface elevation of 1585 m. Lake Ziway is one of the freshwater Rift valley lakes of Ethiopia. It is located at about 161 km south of capital, Addis Ababa, on border between the regions of Oromia and the Southern Nations, Nationalities, and Peoples of Ethiopia. It has a surface area of 434 Km^2 and an elevation of 1846m. Asela located at the Arsi zones of Oromia Region about 175 Kms from Addis Ababa, with an elevation of 2430 m.

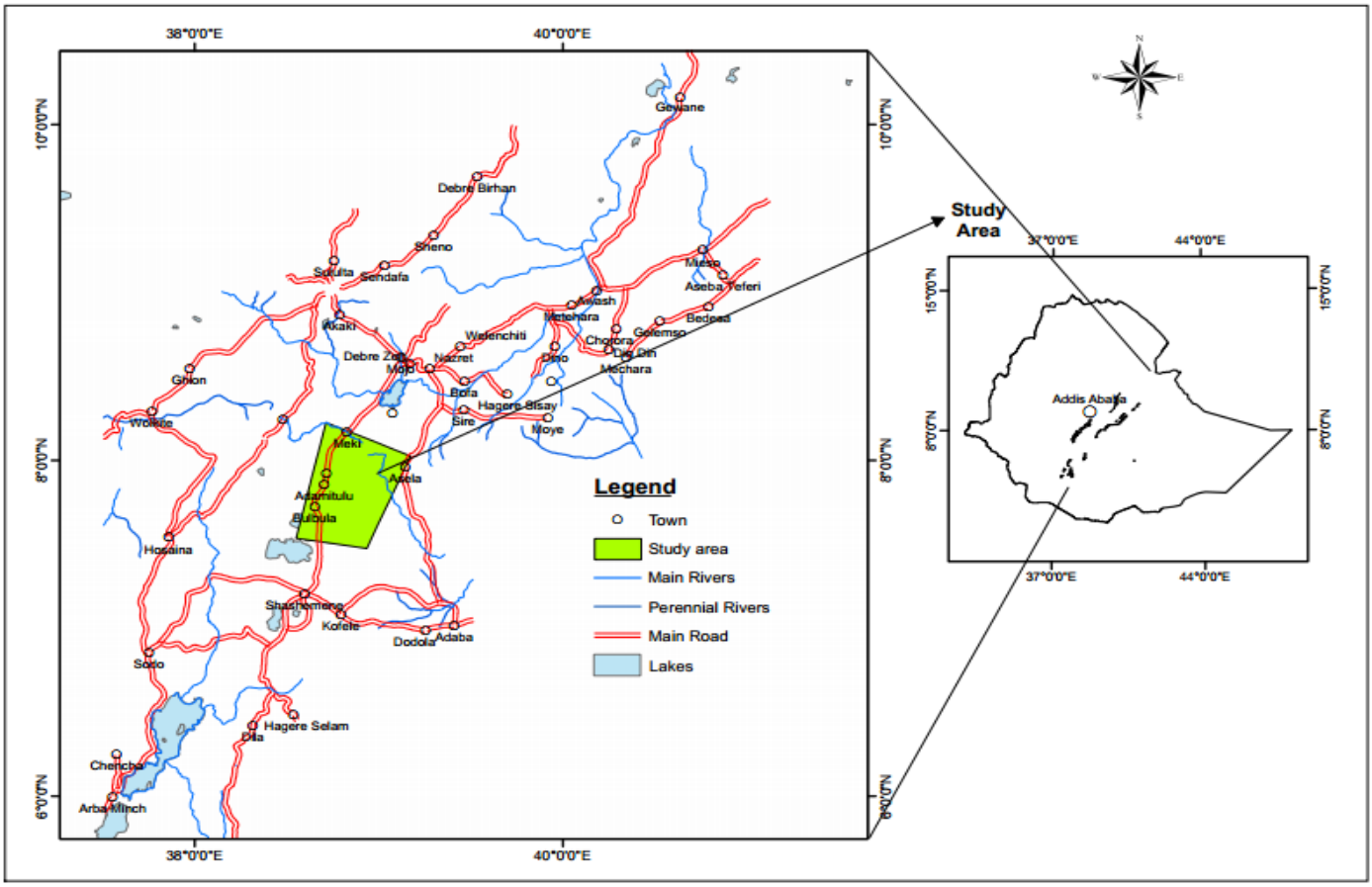

Fig. 1.5 Location map of the study area

1.4 CLIMATE

The Central Ethiopian Rift valley lakes (Ziway, Abyata, Langano and Shala): the rainfall pattern is largely influenced by the annual oscillation of the inter- tropical convergence zone, which results in warm, wet summers with most of the rainfall occurring from June to September and dry, cold and windy winters. Rainfall in Ethiopia is changeable and subject to large spatial variability, which is largely determined by altitude. Areas above 2500 m may receive 1400-1800 mm per year, mid-altitude regions (600-2500 m) may receive 1000-1400 mm per year, and coastal lowlands generally receive less than 200 mm per year. Mean annual rainfall varies in the valley from approximately 500 mm (weather station at Lake Langano) and 650 mm (weather station Lake Ziway) to 1150 mm on the plateau.

The main rainy season accounts for 70-90% of the total annual rainfall. Minor rain events, originating from moist south-easterly winds, occur between March and May. Due to their nature, these rainfall events are more pronounced in the highlands. The Ziway– Shala basin proper is drier, with average annual rainfall around 700 mm. sparse rainfall data (Sagri, 1998) suggest that areas around lakes Abiyata and Langano are even drier.

1.5 AIM OF THE PRESENT STUDY

This project aims at understanding the tectonics and kinematic effects of Earthquake activities in the eastern margin of central Main Ethiopian Rift (MER). A thorough understanding of the deformation type related to this seismic activity is crucial in the investigation of earthquake hazards. Moreover, a careful geological, structural and geomorphologic study help to assess the deformation type in the area related to earthquake activity. This research is conducted by making a detailed field structural mapping of active faults in the Langano area and adjacent regions. The structural analysis will also be coupled with geomorphological analysis of fault scarps, available GPS observations and kinematic analysis.

1.6 OBJECTIVES

This project is proposed to determine the main tectonic structures and their correlation with seismicity, to map the location and extent of individual faults and fault zones in the Langano area and surrounding region. The specific objectives of this study are the following:

- To study and map deformation pattern and type.
- Geomorphologic analysis of fault scarps. Detail analysis on the reactivation of faults due to multiple earthquake activities.
- Determining local and regional extension directions from inversions of fault data and earthquake focal mechanism solutions.
- Mapping geology of the study area to comment on which geologic units are affected by different structures.

1.7 METHODS AND PROCEDURES

Routine geological and structural geology field methods were employed to decipher the kinematics of the study area.

1.7.1 PRE-FIELD WORKS

At the first steps of the study, different available information about the area and previous works are gathered and evaluated. This section includes reading and organizing different literatures on geology, kinematics and tectonics of the main Ethiopian rift in general; and the eastern margin of central main Ethiopian rift, in particular. Furthermore, detail study on the geological and structural maps are done on different scales (e.g Abebe, 1993; Pizzi et al, 2006).

1.7.2 FIELD ACTIVITIES

The objective of the field work is to take different structural measurements at the field in order to analyze the kinematics and stress field of the fault system in the study area.

Field investigations were designed to collect information on

- Local fault systems
- Morphological characteristics of faults and
- Mapping of geomorphologic markers on faults related to earthquake activities.

1.7.3 POST FIELD WORK

All data collected during the fieldwork are further analyzed and processed. After bringing together all the study outputs the result of the field works are finally drawn and from this the report has to be written.

1.8 THESIS LAYOUT

Chapter one discusses introduction and aim of the thesis project, Discussion on the data acquisition and processing techniques of the study are presented in Chapter two. Chapter three explains the regional geology, tectonic setting and structural framework of Main Ethiopian Rift (MER), with particular emphasis on central MER. Chapter Four is about geology and structure of the study area. Chapter five is about interpretation and discussion on the results of the study and Conclusion and recommendations for further investigations are included in Chapter six.

CHAPTER TWO

2. DATA ACQUISITION

The general objective of the field work is to take different structural measurements at the field in order to analyze the kinematics, stress field and fault structure of the study area.

Field investigations are designed to answer some specific questions regarding

- Identification of local fault networks
- Identification of orientation of faults and
- To get a better knowledge of temporal aspects of faulting which is relevant for the evaluation of seismo - tectonic segments.

The approach on recognizing pattern of structural zones can be done using kinematic analyses of fault structures. Structural elements such as fault slickenside surfaces or striation are common indicators for kinematic analysis of faults. Mapping of the eastern margin of fault zone structures has carried out at thirteen traverses and the geometry and kinematics of the faults shown in detail.

Field data collected includes:

- spatial orientation of fault surfaces and striations
- relative movement on fault surface, accompanying fractures and displacement of older structures and
- The rock type which accommodate kinematic indicators

Distribution of fault trends and kinematics in the traverses show that the fault mapped in the area striking in NNE to SSW, NNW to SSE, NE to SW and ENE to WSW Direction. The majority of faults are steeply dipping with about an average of 75 degrees. A study area is characterized by almost ignimbrite of excellent exposure which are affected by tectonic activities and they show well the faults of the area.

The equipment used for data collection during geological fieldwork consisted of Differential Global Positioning Satellite receiver (GPS), Brunton Compass and a digital camera. Twenty eight fault-slip indicators were measured. Each fault-slip measurement consists of the strike/dip of the fault plane, the dip direction and rake of fault slip indicator.

Table 2.1: Structural data collected from field

Location	**Strike**	**Dip**	**Dip direction**	**Rake**
N =8^0 3.968' E =39^0 7.066'	15	75	105	75
N= 7^0 58.313' E= 38^0 02.974'	355	70	85	-86
N =7^0 58.172' E = 39^0 2.879'	350	72	80	-85
	345	77	75	-85
	350	70	80	-85
N =7^0 57.598' E = 39^0 2. 165'	337	65	67	-80
N=7^0 56.733' E =39^0 59.506'	65	82	155	-80
	60	84	150	85
	55	72	145	85
N= 7^0 52.358' E = 39^0 1.736'	27	70	297	85
N =7^0 50.670' E =39^0 0.235'	35	75	305	87
	43	64	313	85
	45	70	315	80
	35	67	305	88
	28	75	298	87
	22	76	292	82
	32	80	302	87
	15	85	285	90
	30	82	300	-85
N =7^0 50.096' E =38^0 59.858'	30	85	300	-80
	35	83	305	-85
	35	87	125	-80
N =7^0 48.553' E = 38^0 58.530'	67	78	337	-84
	50	72	320	-85
	20	75	290	-85
	35	82	305	85
	60	65	330	-85
	47	70	317	-86

2.1 DATA PROCESSSING TECHNIQUES

For the purpose of characterizing the area with the kinematic data, the stress inversion method is applied to the structural datasets using a public domain software FaultKin (Allmendinger et al. 2012). This program does not require a priori discrimination between the active and virtual nodal planes. A total of 28 structural measurements collected during the field survey are used. Below, it is described how FaultKin works and the main frames of the program.

Faultkin is fault slip analysis program for Mac and windows. The main faulkin window is divided into three main sectors. The tab panel on the left shows various types of information about the data set. The four tabs are:

- The **plot tab** shows all of the graphical plot of data. What appears here is controlled by what items are checked in the Plot Menu.
- The **data tab** shows all of the attributes assigned to the first datum selected in the data list box. All editing of data is done in the Data Tab. Changes are not recorded until click the "Calculate and Save" button in the Data tab.
- The **select tab** is where you define searches to select a subset of your data based on multiple criteria. Searches toggle on or off the checkbox next to each datum in the Data List box.
- The **map tab** will plot selected faults on Google satellite, hybrid, terrain, or road map. This image can be saved by dragging it to the desktop.

The **Data List box** gives a listing of the basic data for data set. The values shown here cannot be edited in the list box; editing must be done in the Data tab. Data are sorted by slicking the header of the column by which you want to sort. Sorting does not change the number of each datum (i.e. the number shown in the first column on the left), just the orders of the rows.

The **Analysis Area** is an editable text field where FaultKin writes the results of the analyses and calculations it carries out copy and paste to this area is possible, write your own notes, and erase what you do not need. The data in this area is not saved when you save a data set so be sure you copy any information you need before closing the program.

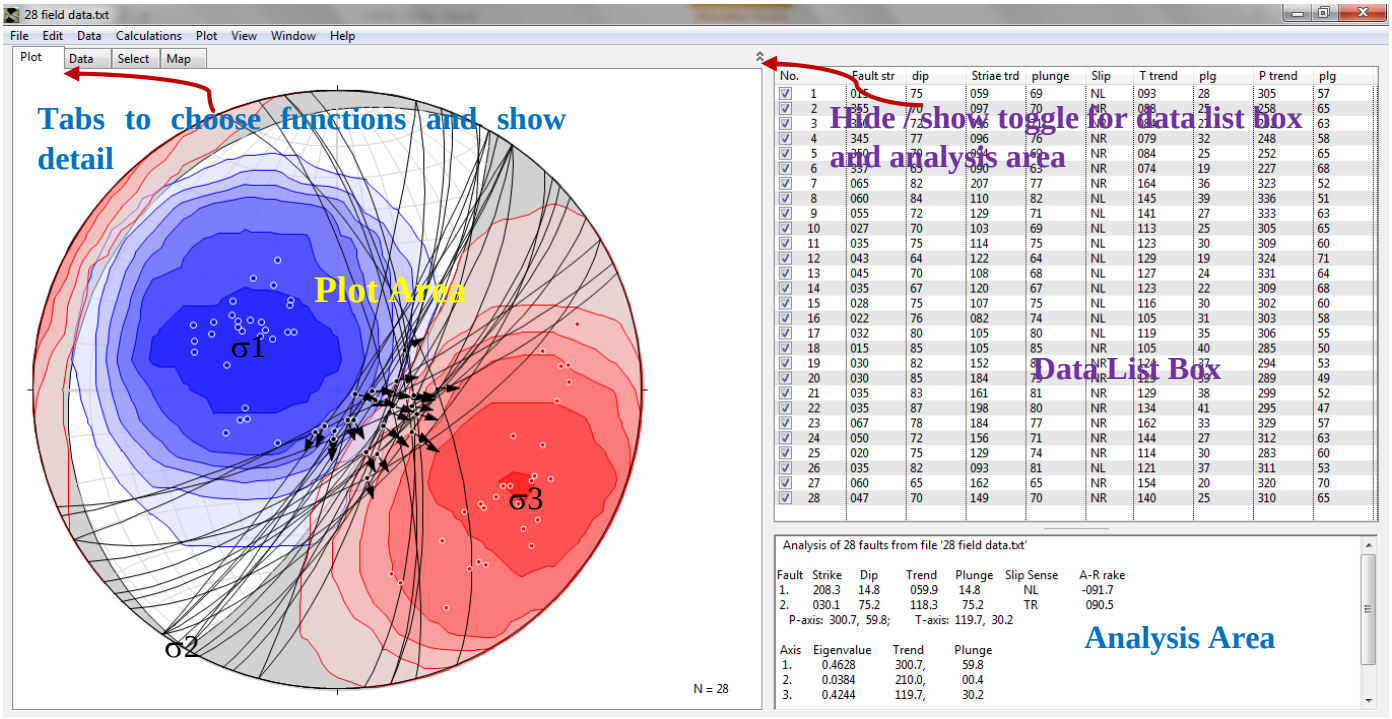

Fig. 2.1 The main fault kin window

The analysis of fault slip data yields information concerning

- Fault movements
- Stress state of the region
- Geometry of fault pattern
- Extension direction
- Regional fault patterns developed to contrast it with the local extension direction

Faults of the area are digitized from Google earth for morph tectonic interpretation of satellite images and this morphotectonic interpretation of satellite images helps so as to analyze fault orientations. The structural studies within selected outcrops carried out based on this standard techniques. The sense of movement was derived from kinematic indicators, striations or slickensides. sigma 1,2 and 3 directions, all fault data are plotted, the two planes auxilary and fault planes are determined to yield fault plane solutions (using FaultKin Allmendinger 2012).

The stress analysis was applied to determine the possibility of reactivation of defined fault sets within the current stress field related to the eastern margin of Central Main Ethiopian Rift. For that reason, we compared the local stress tensors resulting from the analysis of fault kinematic data recorded in the field with the current stress regime obtained from focal mechanism solutions.

CHAPTER THREE

3. REGIONAL GEOLOGY

3.1 GEOLOGY OF MAIN ETHIOPIAN RIFT

The Main Ethiopian Rift is a symmetrical graben with uplifted flanks and steep border faults; it lies between latitude of 5º-9º N and longitude of 37º30'-40º (WoldeGabriel et al., 1990). It is geographically divided into three sub sectors: northern, central and southern sectors (WoldeGabriel et al., 1990) and bordered by the Ethiopian plateau to the west and Somalia plateau to the east. The Main Ethiopian Rift divides the 1,000 km wide uplifted Ethiopian volcanic province asymmetrically into the northwest - southeast plateaus (WoldeGabriel et al., 1990).

Volcanic sequences that cover the area are more voluminous and widespread on the northwest plateau than on the southeastern side (WoldeGabriel et al., 1990). According to WoldeGabriel et al., (1990); Hofmann et al., (1997) the Ethiopian Rift developed within an Eocene-Oligocene flood basalt province.

The Main Ethiopian Rift, like the rest of the East African Rift System, has undergone a very complicated geological evolution and tectonic history. The regional geology of the Ethiopian Rift System has been extensively described and well documented (Mohr, 1962, 1970). The rift valley was the site of extensive volcanic activities during the Tertiary. Volcanic rocks of Pliocene and Pleistocene age such as pantelleritic rhyolite, trachytes, ignimbrites and basalts are abundant within the rift floor and on the adjoining plateaus (Kazmin, 1972). A geological map of central Ethiopia is given in Figure 3.1.

In the northern Main Ethiopian Rift two pre-rift flood basalt episodes predominantly transitional to tholeiitic occurred by 24–23 Ma and 11–8 Ma (the latter characterized by less alkali basaltic shield volcanism) (Chernet et al., 1998). Extension, basin subsidence and rift-flank uplift began during or after the second flood-basalt phase (Ebinger et al., 1993). The Main Ethiopian Rift propagated into the Afar depression after 11 Ma (WoldeGabriel et al., 1990; Wolfenden et al., 2004). Bimodal volcanism (basalt-rhyolite) appeared by ~7 Ma and continued to recent times (Chernet et al., 1998). In the late Miocene and during the Pliocene intra-rift marginal aligned silicic centers developed.

During the Plio Quaternary, volcanism was concentrated within the rift floor (Chernet et al., 1998), and felsic products constitute 80% of the exposed Plio Quaternary rocks in the Main Ethiopian Rift (Mohr, 1983). The oldest (pre-2 Ma) and youngest (post-0.6 Ma) intra-rift units are characterized by bimodal compositions (alkali basalts and rhyolites, mainly pantellerites), whereas in the intervening period (~1.6–0.6 Ma) units occur with unimodal characteristics (pantellerites) (WoldeGabriel et al., 1990). It is assumed that the bimodal compositions indicate a period of increased extension (Boccaletti et al., 1999). Recent basalts (post-0.6 Ma) are essentially fissural and have geochemical signatures characteristic of Mid Oceanic Ridge Basalt (Seth et al., 2005).

Geology of central Ethiopia is classified under six litho-units (Abebe et al., 2010). These lithologies are described below:

3.1.1 Pre -Tertiary sediments and crystalline basement

Despite the occurrence of widespread faulting, subsidence and uplifting related to the formation of the MER, the pre-rift geology is barely exposed along the rift system (Woldegabriel et al., 2002). The boundary faults expose crystalline basement rocks beneath tertiary volcanic rocks in the southern sector of the MER, whereas in the central and the northern sectors, the rift margins are tertiary mafic and silicic rocks. Pre-Tertiary crystalline basement and Mesozoic sedimentary rocks that are unconformably overlain by Oligocene to Pliocene basalt flows and silicic tephra are exposed in the western margin of the central sector at the Guraghe Mountains (Woldegabriel et al., 1990).

The western rift of Guraghe escarpment exposes a silver of crystalline basement with its cover of Mesozoic sedimentary strata, and a 1.5 km thick section of basalt dominated volcanic rocks (Di Paola, 1972) along several step faults. The crystalline basement is represented by an altered biotite gneiss intruded by swarms of northwest trending quartzo-feldspathic pegmatites. The Mesozoic sequence, which is widely present across Ethiopia, uncomformably overlies the crystalline basement at Guraghe.

3.1.2 Oligocene (32–29 Ma) and lower Miocene (12–8 Ma) plateau volcanics

This is the oldest volcanic unit in the central sector of Main Ethiopian Rift and is found at Agereselam and Ambo, Welkite and Chilalo shield volcano. These Oligocene rocks are dominated by basalt with localized rhyolite and sedimentary strata (Woldegabriel, 1990).

The main part of the Ethiopian plateau volcanics consists of the Trap Series (Hofmann, 1997; Pik et al., 1998; Ukstins et al., 2002) and are in age of 32-29 Ma. They cover an area of more than 600, 000 km^2 and locally reaches thicknesses exceeding 3000 m (Mohr and Zanettin, 1988). After a long period of ~11-8 Ma age less voluminous and more local volcanic activity related to the development of shield volcanoes (Corti, 2009), basaltic–trachytic lava flows and associated pyroclastics were formed. They constitute the largest part of the Guraghe escarpment and extend for several tens of kilometers west of the escarpment.

Their average thickness at the Guraghe margin is 600–700 m. Rocks of this volcanic succession are also absent at the Kella block. For both volcanic events widespread time-correlative basaltic units occur on the western and eastern margins of the Central MER, constraining the lateral extent of these events. New K–Ar ages from along the well-exposed volcanic sections of the Guraghe margin and the Ghibe river canyon, located 75 km west of the Guraghe rift margin.

3.1.3 Miocene–Pliocene rift-shoulder trachytic–rhyolitic volcanics and pyroclastic layers

Several layers of pyroclastic rocks associated with trachytic and rhyolitic lava domes and flows together with some important central volcanoes were formed in this episode, and cover the MER shoulders and floor. The products of this episode consist of uncompacted pumiceous fall and flow deposits, rhyolitic–trachytic lava flows forming central volcanic edifices, fissural basaltic lava flows with associated scoria and phreatomagmatic cones, and interbedded lacustrine deposits.

Radiometric ages from both the eastern and the western margins of the MER range between 5.2 and 2.6 Ma. These highly differentiated central and⁄or fissural effusive and explosive eruption products indicate that volcanic activity during this period was very intensive and vigorous.

3.1.4 Plio-Pleistocene rift floor

The rift valley was the site of extensive volcanic activities during the Tertiary. Volcanic rocks of Pliocene and Pleistocene age such as pantelleritic rhyolite, trachytes, ignimbrites and basalts are abundant within the rift floor and on the adjoining plateaus (Kazmin, 1972).

The eastern margin is covered by Pliocene to early Pleistocene (4.6-1.6Ma) shield volcanoes (Chilalo, 4005m; Kekha 4245m; Badda, 4170m). These consist of trachytes with subordinate basalt (Di Paola., 1972; Merla et al., 1979; WoldeGabriel et al., 1990; Bigazzi et al., 1993). Silicic

pyroclasic materials cover most of the MER floor (Mohr, 1962; Di Paola, 1972; WoldeGabriel et al., 1990); they are Early to Middle Pliocene (4.2-3Ma, WoldeGabriel et al., 1990), mainly peralkaline rhyolitic ignimbrites interlayered with basalts and tuffs.

3.1.5 Quaternary central volcanics and basaltic lava flows, associated scoria cones and phreato-magmatic deposits

Quaternary volcanic activity was spatially associated with the oblique faults of the Wonji Fault belt affecting the rift floor and still characterized by both silicic rocks (Bora-Bericha Rhyolites Of Abebe et al.[2005]) and basalts (Wonji Basalts of Abebe et al. [2005]). Silicic rocks form large central volcanoes, some characterized by well-developed calderas, which give rise to ignimbrites, lava flows, domes and phreatomagmatic deposits, with compositions ranging from trachyte to per-alkaline rhyolites; basalts form small lava flows, scoria cones and phreatomagmatic deposits. Radiometric ages of this activity are generally <1.8 Ma [e.g. WoldeGabriel et al., 1990; Abebe et al., 2005], whereas the last eruptions are estimated to be Holocene in age.

3.1.6 Quaternary lacustrine sediments and interbedded pyroclastics

In the Quaternary (<1.6–1.8 Ma), bimodal volcanic rocks (lava, pyroclastics and volcanoclastic strata) were generally closely associated with Wonji Fault Belt affecting the rift floor [e.g., WoldeGabriel et al., 1990]. North of Lake Abijata, a great thickness of late Quaternary lacustrine and fluvial sediments is exposed by the Bulbula River and its tributaries. These sediments have been referred to as the Bulbula Formation (Street, 1979).

Pleistocene -Holocene lacustrine sediments cover a significant tract of ground and were deposited in a huge lake whose level before 3500 to 2100 years used to be 100m higher than its current level (Kazmin et al., 1980). In the rift floor, interlayering of primary air fall pryroclastic deposits and lacustrine deposits are common. The subaqueous pyroclastic deposits can be identified by reverse graded bedding of pumice layers. Rounded rock fragments indicating abrasion during transportation by rivers and waves of lakes, poor consolidation, and presence of evaporites distinguish subaqueous pyroclastic materials form reworked sedimentary deposits. Evaporites such as soda or trona (NaHCo3) and micro -organic (diatomite) deposits occur around Lake Ziway, North of lake Abiyata, the sediments attain a thickness of 600m.

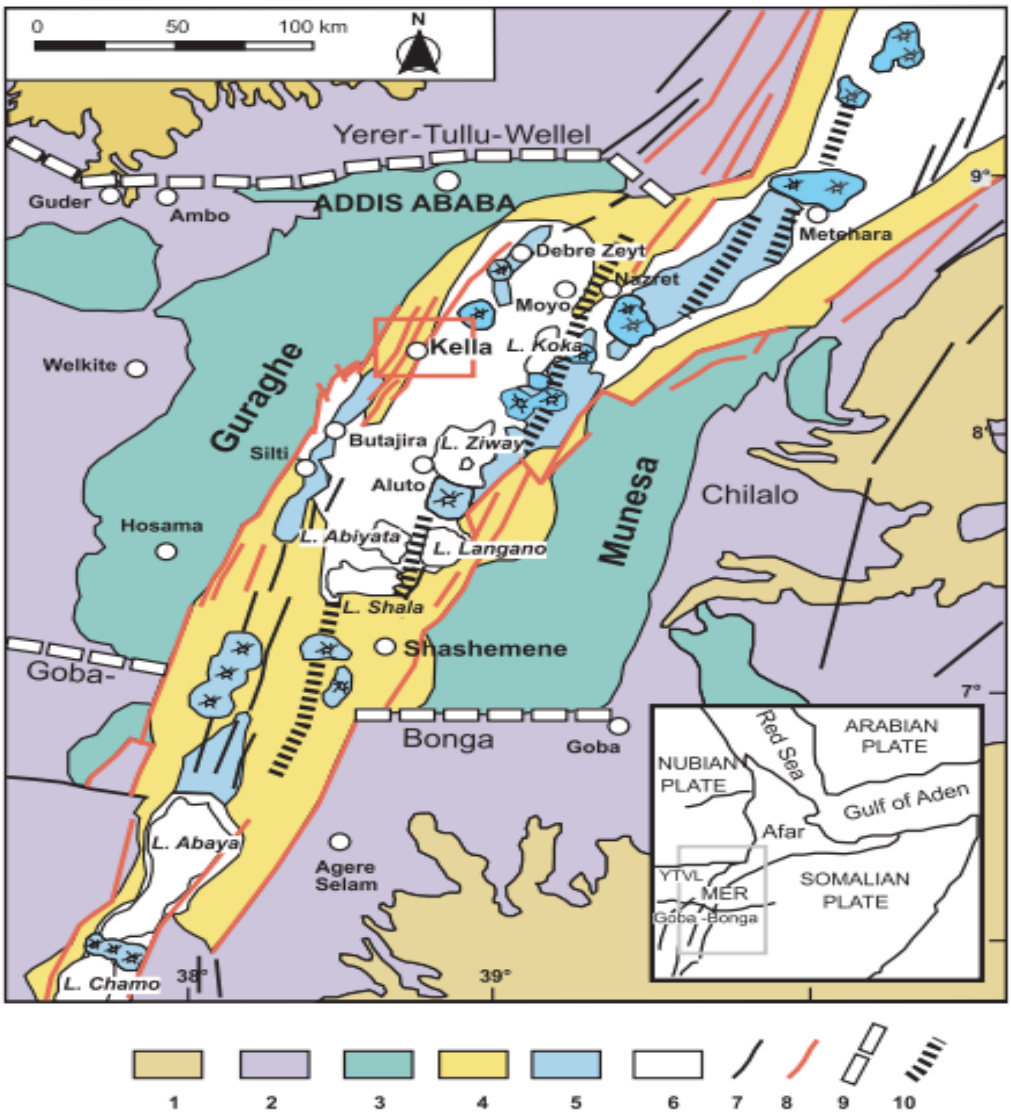

Fig. 3.1 Simplified geological map of central Ethiopia

(1) Pre-Tertiary sediments and crystalline basement, (2) Oligocene (32–29 Ma) and lower Miocene (12–8 Ma) plateau volcanics, (3) Miocene–Pliocene rift-shoulder trachytic–rhyolitic volcanics and pyroclastic layers, (4) Plio-Pleistocene rift floor, (5) Quaternary central volcanics and basaltic lava flows, associated scoria cones and phreato-magmatic deposits, (6) Quaternary lacustrine sediments and interbedded pyroclastics, (7) faults, (8) major rift border faults, (9) major transversal tectonic lineaments in the basement, (10) Wonji Fault Belt segments. Red square: area show Kella area. In the inset: YTVL, Yerer-Tullu-Wellel volcanotectonic lineament, MER, Main Ethiopian Rift.

3.2 TECTONIC SETTING OF MAIN ETHIOPIAN RIFT

The Main Ethiopian Rift is part of the East African Rift System (EARS) that extends from the afar triple junction in the north, to the Turkana Rift in the South (Agostini et al., 2011). The Main Ethiopian Rift progressively widens northward. This widening is associated with a decrease in the length of its rift segments, of the separation of magmatic centers, and of the effective elastic thickness of the crust (Ebinger and Hayward, 1996). The rift started to develop during the Miocene (Davidson and Rex, 1980; WoldeGabriel et al., 1990; Chernet et al., 1998), following a broad doming centered on the present Afar depression (Almond, 1986; Ebinger et al., 1989; Collet et al., 2000; Benoit et al., 2006).

During the Pliocene and Quaternary, the Main Ethiopian Rift progressively deepened, evolving through a sequence of interacting half-graben segments marking the boundary between the Nubia and Somalia Plates (Hayward and Ebinger, 1996).

The youngest part of the Main Ethiopian Rift is the axial zone, or rift axis, which coincides with the so called Wonji Fault Belt, (which mainly formed during the Quaternary (Mohr, 1967, 1987; Boccaletti et al., 1998; Corti, 2008). Wonji fault belt is characterized by active NNE-SSW–trending extension fractures and normal faults. The WFB is a tectono-volcanic system characterized by short, closely spaced, active faults that exhibit minor vertical throw, which developed essentially in the last 2 my (e.g., Boccaletti et al., 1999; Ebinger and Casey, 2001). These are often set in a right-stepping en-echelon arrangement and are associated with volcanic activity, suggesting a possible overall left-lateral component of motion along the Wonji fault belt (Bonini et al., 1997).

The Wonji Fault Belt obliquely cutting the rift floor are believed to accommodate the majority of current deformation, as indicated by GPS measurements [Bilham et al., 1999; Bendick et al., 2006] and analysis of the current seismicity (Keir et al., 2006). The slightly different trends of the WFB and the Main Ethiopian Rift margins suggest a change in the extension direction during the Quaternary (Bonini et al., 1997; Boccaletti et al., 1998). The border faults are normally long, widely spaced and characterized by large vertical offset and are interpreted to have accommodated the tectonic deformation during the initial stages of rifting (Hayward and Ebinger, 1996; Boccaletti et al., 1998).

The Northern MER is considered to extend from the Afar depression up to the Lake Koka region following the middle course of the Awash River valley (Bonini et al., 2005). The northern MER shows two well-developed fault systems, (1) the border faults and (2) a set of faults affecting the rift floor, usually referred to as Wonji Fault Belt (e.g., Mohr, 1962; Chorowicz et al., 1994; Boccaletti et al., 1998; Acocella et al., 2003). On the basis of seismicity (Keir et al., 2006) and local geological data (Wolfenden et al., 2004; Casey et al., 2006) the border fault set is thought to have been deactivated and mostly eroded in the northern MER.

The main boundary faults in this region show an average $N50^0$ trend [Kazmin et al., 1980; Mohr, 1983; Hayward and Ebinger, 1996; Chernet et al., 1998; Wolfenden et al., 2004]. The activation of these faults is diachronous along the rift axis; in the NMER it is commonly interpreted to have occurred in the Late Miocene (~11 Ma; Wolfenden et al., 2004). Geophysical data indicate crustal thinning and strong tectonomagmatic modifications of the crust and lithosphere in the northern MER, with magma intrusion emplaced throughout the lithosphere below the WFB where deformation is currently accommodated by a combination of intrusion, dyking and normal faulting [Keir et al., 2006, 2009]. The WFB is thus interpreted to accommodate a phase of magma- assisted rifting during the late stages of continental rifting (e.g., Kendall et al., 2005; Bastow et al., 2010).

The WFB faulting developed essentially in the last 2 my (e.g. Boccaletti et al., 1999; Ebinger and Casey, 2001) and was intimately associated with the intense Quaternary magmatism in the rift floor. These faults are well developed in the NMER and the occurrence of WFB fault system decreases southwards.

At Central MER the main boundary faults trend roughly $N30^0$–35^0 E. The activation of faults at the CMER is from Late Miocene–Early Pliocene (~6–8Ma; Bonini et al., 2005; WoldeGabriel et al., 1990). The Southern MER occurred at Plio-Pleistocene which extends south of Lake Awasa into the ~300 km-wide system of basins and ranges referred as broadly rifted zone [Davidson and Rex, 1980; Ebinger et al., 2000] that characterizes the overlapping area between the Ethiopian and Kenya Rifts. Faults in the Southern MER show a dominant N-S to $N20^0$ trend were well established after ~18 Ma (Levitte et al., 1974; Zanettin et al., 1978; WoldeGabriel et al., 1991; Ebinger et al., 1993), whereas volcanism started in the early Miocene around 18–21 Ma (Levitte et al., 1974; Zanettin et al., 1978; Ebinger et al., 1993; George and Rogers, 2002).

In the central and southern MER sectors boundary faults are well developed, and analysis of historical seismicity (Gouin, 1979; Keir et al., 2006) and scattered geological data (Pizzi et al., 2006) suggest that at least part of these faults may be active. There is a decrease in the tectonomagmatic modification of the crust and lithosphere proceeding from the northern MER sector southward [e.g., Keranen and Klemperer, 2008], which accords with a southward decrease in rift evolution. Wonji faults are well developed in the NMER than Central and southern MER; At the central MER, deformation is mostly localized nearby both rift margin as compared to the northern MER where most of deformation is localized in the center of the rift, along the volcano tectonic WFB segments .

The three segments as representing different stages of the extension process, from early rifting in the Southern MER to more evolved stages in the Central and Northern MER preceding the incipient seafloor spreading in Afar (Hayward and Ebinger 1996).

According to Abebe et al., (2010) the main rifting phase in the Central MER took place after 8 Ma, as deformation in the Northern MER started at 11 Ma (Wolfenden et al., 2004), postponing the formation of the Central MER to after 8 Ma means that the different MER segments actually formed at different times. Extensional structures started to develop in the Southern MER during the Early Miocene (20–21Ma) due to the northward propagation of Kenya Rift-related deformation. A further propagation towards the north was probably hindered by inherited transversal lines, such as the Goba-Bonga lineament. In the Late Miocene (11–8 Ma) the deformation, propagating southwards from the Afar, focused on the northern MER, while the Southern MER became essentially inactive. At that time no major extensional deformation was yet affecting the Central Main Ethiopian Rift.

Significant extensional deformation and rift opening are evident for the Central MER at the boundary between the Miocene and Pliocene, with high volcano-tectonic activity after 5 Ma. Finally, from 3 Ma to the Present, propagation of the MER towards the south probably reactivated the older rift structures in the Southern MER (Bonini et al., 2005) attributed the opening of the Central MER and the Quaternary reactivation of the Southern MER to the southward propagation of rifting induced by the clockwise rotation of the Somalian plate starting at about 10 Ma (Collet et al., 2000). The tectonic setting in which the MER developed well after the beginning of rifting in the Gulf of Aden (>20 Ma) points to a diachronous development of the Red Sea–MER–Gulf of Aden area. The third arm of the triple junction nucleated in the Afar after 11 Ma (Wolfenden et al.,

2004) and then, according to the Bonini et al. (2005) propagated southwards. The tectonic setting of the three MER sectors are given in Figure 3.2 below.

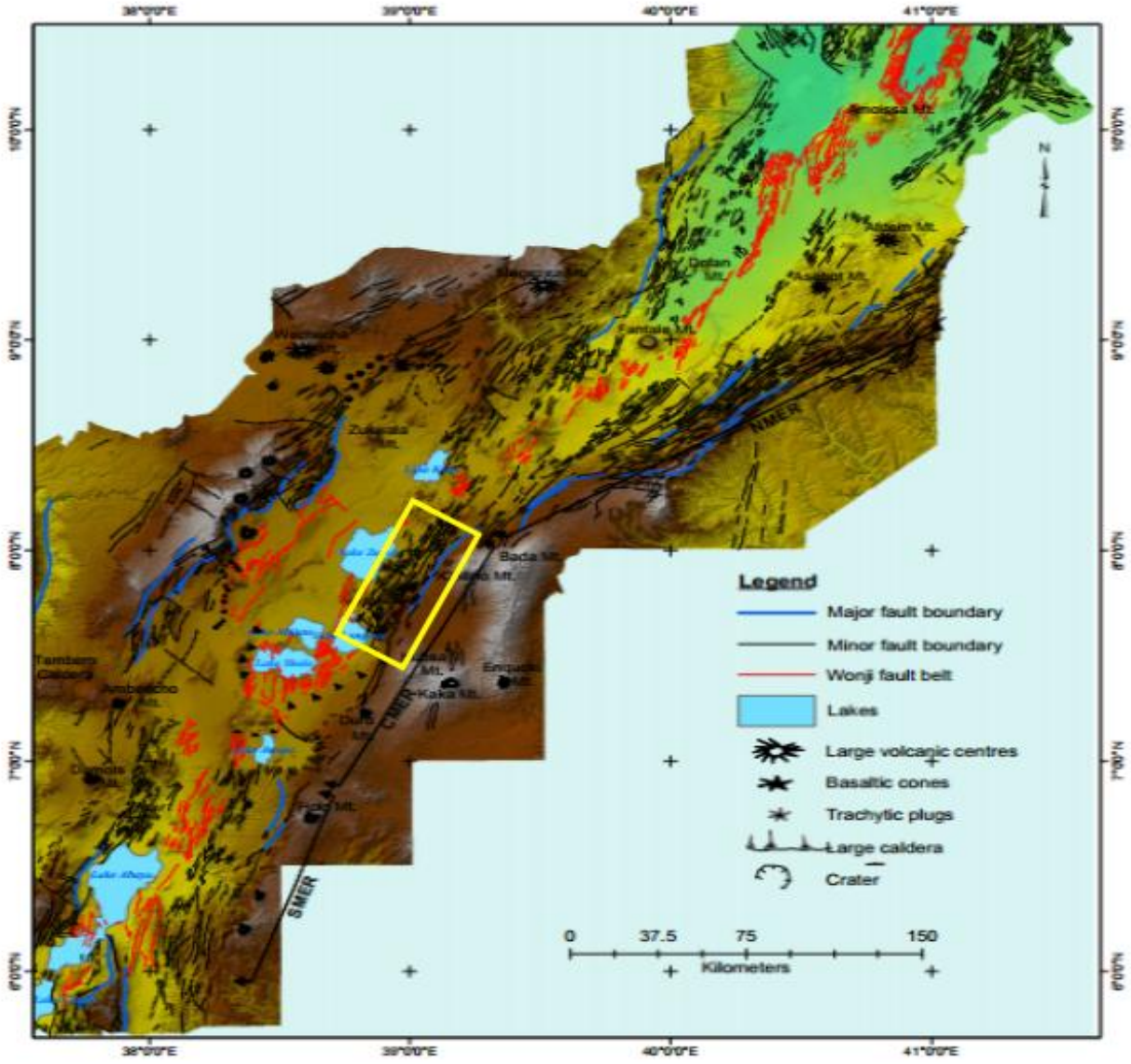

Fig. 3.2 Tectonic sketch map of the Main Ethiopian Rift (modified after Boccaletti et al., 1998) superimposed on Digital Elevation Model. SMER (southern main Ethiopian rift), CMER (central main Ethiopian rift), NMER (northern main Ethiopian rift). WFB show the en-echelon, right-stepping arrangement of the volcano-tectonic segments. The yellow rectangle represents the study area.

3.3 STRUCTURAL FRAMEWORK OF MAIN ETHIOPIAN RIFT

The East African Rift System (EARS) is one of the largest continental rift systems on the Earth which provides an opportunity to investigate the compositional variation of erupted magma with the amount of extension. The East African Rift System is a Miocene- Quaternary intra-continental extensional system, divided into Eastern and Western branches and composed of several interacting segments from Mozambique to Afar (Davidson and Rex, 1980).

The Main Ethiopian Rift is a NNE-SSW trending rift valley: it represents an ideal place to analyze the progressive evolution of continental extension, as it may encompass the transition from border fault-controlled to localized strain within the central rift valley (e.g., Hayward and Ebinger, 1996; Corti, 2009).

Most of the recent Quaternary volcanic activity in the MER is closely associated with the Wonji faults. The recent alluvial cover and volcanic rocks are affected by this fault system, therefore, accommodates Holocene deformation (e.g., Boccaletti et al., 1998). Although a roughly NW–SE extension has been deduced from the analysis of open fractures within different Wonji segments (Acocella and Korme, 2002). The right-stepping en-echelon fault arrays, the complex pull-apart structures suggests that this fault system accommodates a left-lateral, oblique shearing along the rift axis resulting compatible with a roughly E–W oriented extension (e.g., Bonini et al., 1997; Boccaletti et al., 1998; Pizzi et al., 2006; Kurz et al., 2007).

According to Agostini et al., (2011) in the NMER, the internal WFB faults, well organized in en-echelon segments, are higher in number than the border faults, being the border faults over internal faults ratio is 0.57. The border faults consist of long and spaced en-echelon structures (average length 1.80 km, maximum length ~25 km, average spacing 1035 m), whereas the internal faults are shorter (average length 1.26 km, maximum length ~15 km) and more closely spaced (955 m on average).

In the CMER and SMER, the border faults over internal faults ratio shows high values (4.38 and 5.20, respectively) thus manifesting the clear predominance of the border faults. These latter are longer (2.56 km and 2.64 km in the CMER and in the SMER, respectively) and more spaced (1200 m and 1260 m in the CMER and SMER, respectively) compared with the northern sector. Qualitatively, the internal faults in the CMER and SMER sectors appear as short structures (only a

few faults are longer than 10 km) with small vertical separation (e.g. Boccaletti et al., 1998), resulting individually similar to those in the NMER.

Qualitatively, the internal faults in the CMER and SMER sectors appear as short structures (only a few faults are longer than 10 km) with small vertical separation (e.g. Boccaletti et al., 1998), resulting individually similar to those in the NMER. Nevertheless, the en-echelon arrangement of the NMER internal faults is not clearly detectable in the CMER and SMER, where internal faults are concentrated mainly near the rift margins, and only few of them affect the center of the rift valley.

The differences observed in the fault pattern and in the distribution of deformation along the different MER suggest along-axis variation in rift evolution. A north to south variation of fault pattern reflects a different distribution of the brittle deformation across the rift structure: in the NMER faulting affects primarily the rift depression with the well-developed WFB, while deformation in the CMER and SMER is concentrated on the rift margins.

3.4 GEOLOGY AND STRUCTURE OF CENTRAL MAIN ETHIOPIAN RIFT

3.4.1 GEOLOGY OF CENTRAL MAIN ETHIOPIAN RIFT

The central sector of the Main Ethiopian Rift and its shoulders are made of volcanites and pyroclastic rocks, whereas large areas of the rift floor are covered by volcano-lacustrine and fluvio-lacustrine deposits. Limited outcrops of Precambrian biotite gneiss, covered by Early Mesozoic fluvial sandstones, marine shales and limestones, occur in a complex horst structure on the western margin (e.g. Kela horst, Woldegabriel et al., 1990; Di Paola et al., 1993).

Late Quaternary fluvio-lacustrine sediments cover a large area of the central sector of the MER (Merla et al., 1979). They were laid down in a very wide lake which, in the past, occupied most of the rift floor. The four lakes (Ziway, Langano, Abiyata, Shala) are the remnants of that ancient lacustrine basin.

The oldest volcanic rocks are exposed in the western escarpment and consist of about 1000 m of basaltic lava flows, with inter bedded ignimbritic beds, topped by massive rhyolites and intervening tuffs and basalts (Di Paola, 1972; Merla et al., 1979; Woldegabriel et al., 1990; Di Paola et al., 1993). Radiometric ages range from 40 to 25 Ma in the basalts and from 37 to 27 Ma in the rhyolites (Merla et al., 1979; Woldegabriel et al., 1990). Middle Miocene to Pliocene (15–3 Ma) basalt flows,

rhyolites and tuffs unconformably cap the early Tertiary volcanic units (Merla et al., 1979; Woldegabriel et al., 1990).

The eastern plateau is covered by Pliocene to early Pleistocene (4.6–1.6 Ma) shield volcanoes (Chilalo, 4005 m, Kecha, 4245 m Badda, 4170 m). These consist of trachytes with subordinate basalts and mugearites (Di Paola, 1972; Merla et al., 1979; Woldegabriel et al., 1990; Bigazzi et al., 1993), and of Miocene phonolites (Chike Mountain). Silicic pyroclastic materials cover most of the MER floor (Mohr, 1962; Di Paola, 1972; Woldegabriel et al., 1990); they are Early to Middle Pliocene (4.2–3 Ma, Woldegabriel et al., 1990), mainly peralkaline rhyolitic ignimbrites, interlayered with basalts and tuffs and associated with layered, unwelded pumices.

Alkaline and per alkaline rhyolitic lava flows and domes, associated with pumice and ash represent the late silicic volcanic events (Di Paola, 1972). A more recent volcanic unit, crops out along the Silti-Debre Zeit Fault Zone (SDZFZ) and the WFB (Di Paola, 1972; Kazmin et al., 1980); it is made up of basaltic lava flows, associated with hyaloclastites and scoria cones. It is very recent, as testified by a radiometric age of 0.13 Ma (Woldegabriel et al., 1990) and by sub-historical lava flows (Di Paola, 1972; Di Paola et al., 1993).

Young volcanoes and calderas, such as the Bora – Bericcio complex, the Alutu volcano, the Ficke, O'a and Corbetti calderas, are made up of rhyolitic lava flows, unwelded pumice flows, pumice falls and ashes. Obsidian flows represent the final product of the volcanic activity (Di Paola, 1972; Mohr et al., 1980). These recent volcanoes started to be active from the Middle Pleistocene (about 0.25 Ma, Di Paola, 1972; Mohr et al., 1980; Woldegabriel et al., 1990) with intermittent Late Holocene activity; obsidian flows and pumices were dated 2000 y BP (Gianelli and Teklema-riam, 1993) and very recent ash deposits 1500 and 230 y BP (Haynes and Haas, 1974). Many of these volcanoes are presently in a fumarolic stage (Di Paola, 1972). Within the volcanic and volcaniclastic succession of the O'a caldera, Middle Pleistocene fluvio - lacustrine sands and clays occur (Mohr et al., 1980; Le Turdu et al., 1999).

3.4.2 STRUCTURAL SETTING OF CENTRAL MAIN ETHIOPIAN RIFT

In the Central MER, the rift valley orients between N25°E and N45°E and is characterized by major rift escarpments on both western and eastern margins; boundary faults show an average trend around N30°E (Corti, 2009). Some differences in the tectonic lineaments between the eastern and the western escarpment exist; the western margin is well expressed by the N 25°E–N 35°E-trending and ESE-dipping Guraghe and Fonko faults, whereas the eastern margin is well represented by the N30°E-trending and WNW-dipping Asela–Langano fault system. Both systems are characterized by high-angle (N60°) normal faults, with large cumulative vertical throw. Overall, these fault systems give rise to a roughly symmetric rift valley. The structural setting of central main Ethiopian rift is given in Figure 3.4.

The border fault systems are normally segmented and articulated, and characterized by the presence of minor transversal structures and local complex geometries. Near Lake Langano the NE–SW trending border faults curve to acquire a local NW– SE trend and the interaction between these two intersecting trends result in the typical S- or Z-shaped pattern of the Langano (or Haroresa) Rhomboidal Fault System which is shown in Fig. 3.3 (e.g.,Mohr, 1987; Boccaletti et al., 1998; Le Turdu et al., 1999).

Western rift margin is characterized by the presence of roughly N–S-trending structural highs such as the Boru Toru and Midre Kebd structural highs; where lowermost syn-rift volcanic units crop out, which give rise to major embayment's in the rift structure (Abebe et al., 2005). This is evident in the Debre Zeyt area, where the NE–SW-trending rift margin and the N–S Boru Toru structural high give rise to the major Addis Ababa embayment. The presence of these N–S structural highs and embayment's define lacustrine sub-basins that are aligned along N–S trend (Abebe et al., 2005).

Fault-slip data on both rift margins in the Central MER indicate a stress field characterized by an extension direction oriented roughly ESE–WNW, with local variations between E–W and NW–SE (Boccaletti et al., 1992, 1998; Abebe, 1993; Korme et al., 1997; Acocella and Korme, 2002; Bonini et al., 2005; Pizzi et al., 2006).

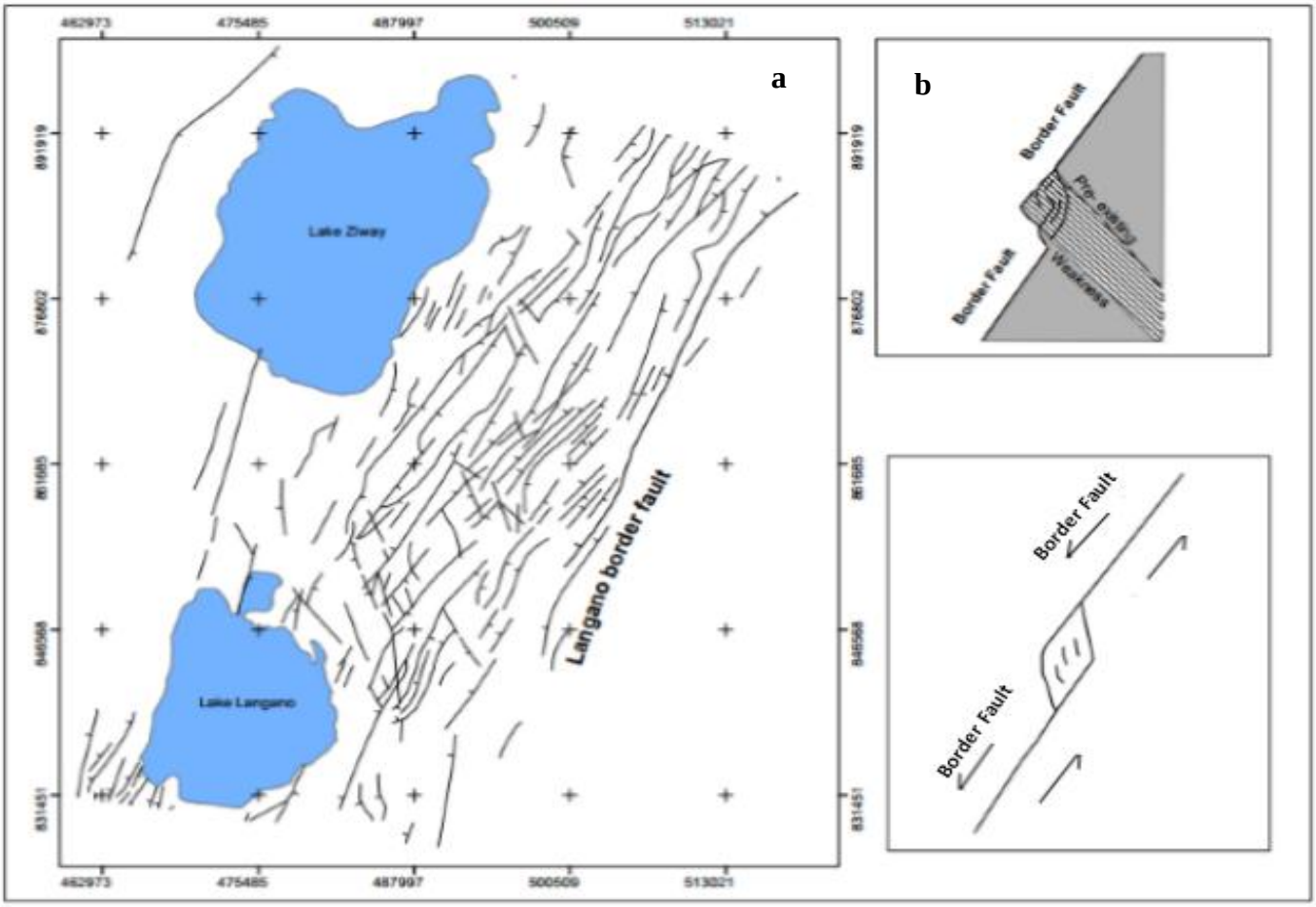

Fig 3.3 Fault pattern in the Langano (or Haroresa) Rhomboidal Fault System. The interaction between NE–SW and NW–SE-trending structures giving rise to the typical S-or Z-shaped fault pattern. b) Models that can explain the development of the rhomboidal fault pattern: upper: influence of a pre-existing NW–SE-trending weakness zone causing a left-lateral offset of the rift margins and the NE–SW boundary faults lower: pull-apart structure related to the left-lateral component of motion along the border fault system (modified after Boccaletti et al., 1998).

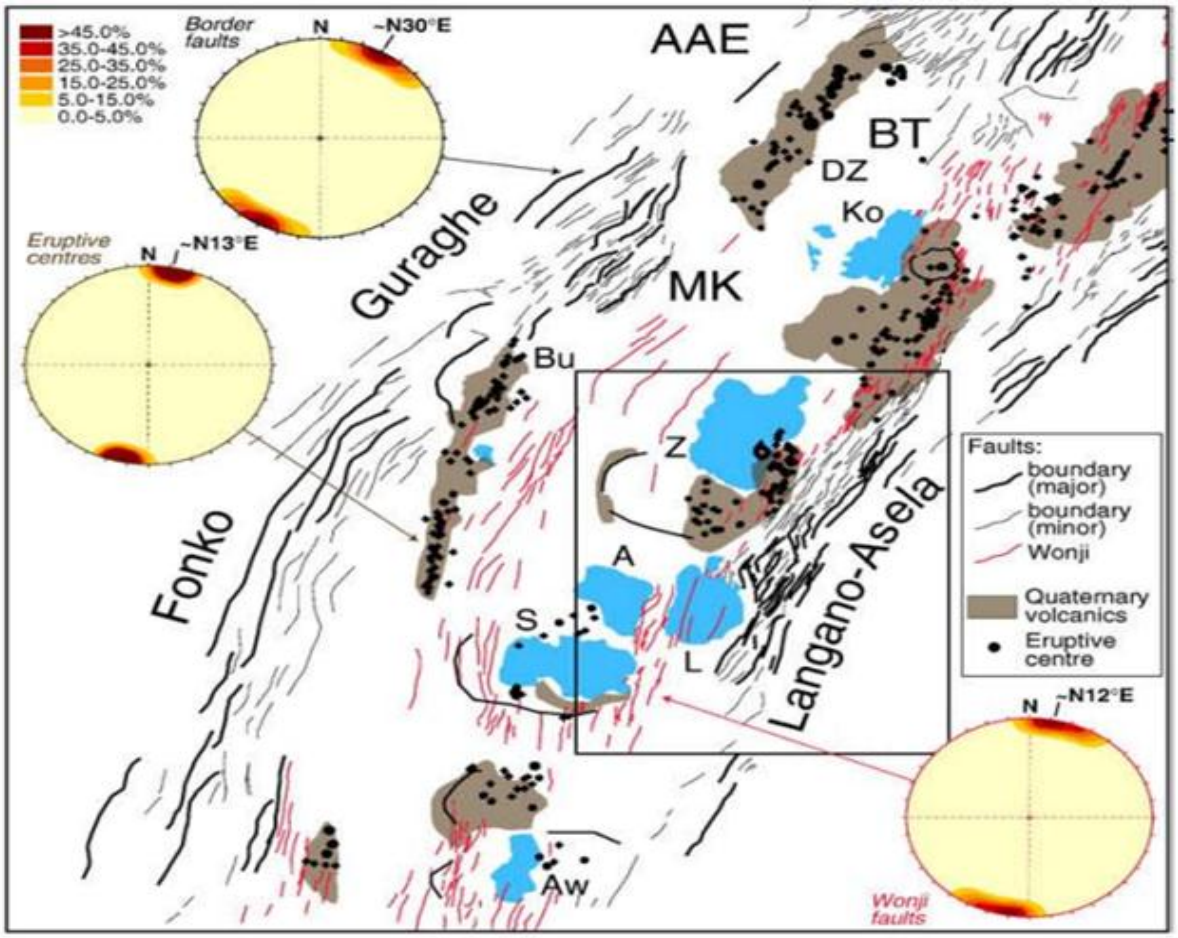

Fig 3.4 Structural setting of the Central MER . A: Lake Abiyata; Aw: Lake Awasa; Bu: Butajira volcanic chain; L: Lake Langano; S: Lake Shala; Z: Ziway.(Corti, 2009). The square represents the easternj margin of central main Ethiopian rift

The most important volcano tectonic event in the central sector of the MER occurred in Early Pliocene, with the eruption of voluminous flows of rhyolitic ignimbrites and the collapse of very large calderas (Di Paola, 1972; Woldegabriel et al., 1990). From early Pleistocene to the present, tectonic and volcanic activity was concentrated along the WFB, and successively along the Silti Debre Zeit Fault Zone (Mohr, 1962; Di Paola, 1972; Bigazzi et al., 1993). Since middle Pleistocene fluvio-lacustrine basins developed along the WFB, under a tectonic– volcanic control (Le Turdu etal., 1999).

CHAPTER FOUR

4. LOCAL GEOLOGY

4.1 GEOLOGY OF THE STUDY AREA

To address the objective of the research, identifications of lithology and associated kinematic indicators are conducted during field work. The lithology of the eastern margin of central main Ethiopian rift is shown in the geological map of the study area (Fig. 4.1) modified from geological map sheet of Geological Survey, Ethiopia.

The lithologic units that make up the geology of the study area consists of late tertiary silicic volcanics (Nazreth Group) overlain by a unit of fissural flood basalt – Bofa Basalt. Chilalo shield volcanoes are also belongs to the late tertiary volcanics which are represented by per alkaline basalt and trachyte. The last major event of rift faulting which has occurred in the quaternary age resulted in the formation of so many volcanic complexes called the Wonji Group. The three major volcanic complexes of the Wonji group are the Dino formation, (stratoid silicics of the rift floor), central volcanic complexes, and the fissural basalts of the rift floor. The youngest stratigraphic succession of the study area is the Pleistocene-Holocene age lacustrine sediments which constitutes most part of the rift floor. Table 4.1 shows the lithostratigraphic succession of the study area with their approximate thickness.

Table 4.1: Lithostratigraphic succession of the study area with their approximate thickness

Period	Age (Ma)	Category	Lithologic Symbols	Thickness (m)	Description
Pleistocene-Holocene	1.5 - 0.8	Quaternary Sediments	Ql	200	Lacustrine Sediment silt, clay diatomites
		Central Volcanic Complexes	Qwa	750	Rayholite with Trachyte Lava flows
			Qwpu	450	Pumice and unwelded tuffs
		Basalts of the Rift floor	Qwbp	250	Pleistocene Basalts mostly vesicular
			Qdi	30	Ignimbrites, tuffs, water lain pyroclastics, lacustrine beds
		Dino formation	N2cb	700	Alkaline Basalts
Pliocene	4.5 - 1.5	Chilalo Volcanics	N2ct	850	Trachyte, basalt peralkaline ryholitic ignimbrites
			Nbb	30	Bofa Basalt: Mildly alkaline Basalts
Upper Miocene-Pliocene	9.2	Nazreth Group	N1-2n	400	Stratoid silicics ignimbrites unwelded tuff, ash flow rhyolite
			NQS	400	Nazreth group and Dino formation undifferentiated

4.1.1 Rhyolite with some trachyte lava flows, pumice and unwelded tuffs (Qwa, Qwpu)

Most of the central volcanoes of the Wonji group are disposed along the axial zone of the rift, the Wonji fault belt. They are either huge conical mountains or calderas formed in the place of older volcanoes. The main volcanic centers from north to south within the rift include Aluto, Shala and Corbetti. The position of some volcanoes and calderas is not so clearly defined. Some occur on the rift floor outside the tensional belts, such as Gademotta caldera, or even on the rift shoulders, such as volcanoes and calderas. Some centers such as Tembero, Wagebeta and Ambericho, show discrete east–west alignment, and may follow transverse faults. The main rock types are rhyolitic and trachytic lava flows (Qwa). In some centers alkaline and per-alkaline products are mainly represented by pumice and unwelded tuffs (Qwpu).

The sequence of eruption of various rocks differs from one volcano to another. Most of the products of central volcanoes are per alkaline rhyolites and trachytes of pantelleritic or locally of comendetic affinity (Di Paola, 1976; Tsegaye et al., 2005).

4.1.2 Pleistocene basalts mostly vesicular (Qwbp)

Another type of volcanic activity in the Wonji Group was the eruption from fissures of Pleistocene basalts (Qwbp). The bulk of these late basalts are concentrated in the Wonji fault belt, but there are also eruptions in the western marginal part of the rift. The basalts are clearly controlled by extensional fractures and generally display fresh aa surfaces. Chains of scoraceous cones follow the lines of fractures. These basalts are exposed at East of lake Ziway, and far North East of lake Abiyata- near Mito town. Recent flows in many cases follow depressions of relief or flow over fault escarpment. The eruption of basalts usually followed the formation of silicic pantelleritic volcanoes, but some basalt might be contemporaneous with the earliest stages of their development.

4.1.3 Ignimbrites, tuffs, water lain pyroclastics, lacustrine beds (Qdi)

The Bofa Basalt and Nazereth Series are in most places overlain by green and gray ignimbrites with well-developed fiamme and associated unwelded pyroclastic and water lain pyroclastic with occasional intercalated lacustrine beds and aphyric basalts. The pyroclastics of the Dino Formation may have sources from axial felsic volcanic eruptions complexes. The felsic lava of the Dino formation are per alkaline in composition and the ignimbrite members are not confined only to the rift floor but extensively developed on the escarpments.

4.1.4 Alkaline basalts, Trachytes, basalts per alkaline rhyolitic ignimbrite (N2cb, N2ct)

Chilalo, Bada, Kubsa, Kaka, and Enquolo are shield volcanoes (Central volcanoes) located on the eastern rift shoulder, marking the water shade of the rift valley lake basin on the east together with Wechacha, Gesh Megal and some others, they belong to a numerous group of complex volcanoes developed in the upper Pliocene on both sides of the rift (Halcrow Group and GIRD 2008.). The two volcanoes found in the study area are Kubsa and Duro. Lava flows of these volcanoes are contemporaneous with the younger ignimbrites of the Nazret group, and partly interfinger with them. The lower complex is composed of intercalating peralkaline ignimbrites and trachytes (N2ct) with clear flow structures in the latter. The upper complex flow is represented invariably by very fresh alkaline basalts (N2cb) commonly with porphyritic structure. In the Duro volcano on the eastern shoulder of the rift only the lower complex (N2ct) is present.

4.1.5 Bofa Basalts: mildly alkaline basalts (Nbb)

Nazreth Group are overlain by a unit of fissural flood basalts which was named after its type locality at Bofa village outside the study area. It is considered to represent the upper part of the stratoid basaltic succession of the Afar Group younger than 4.5 Ma (Kazmin et.al., 1980). The Bofa Basalts form a wedge between the Nazreth and Dino silicics and occur as separate exposures north and east of lake Langano where they are known as ‘Old Rift Basalts’ (UNDP, 1973), and where they finally wedge out. They represent an event of fissural eruption which immediately followed a major faulting event (Kazmin and Seife, 1978, Kazmin et al., 1980).

The fissural basalts of this unit are aphyric locally vesicular and generally form several well defined flows with scoraceous surfaces, in places separated by paleosoils. The rocks are generally weakly

porphyrtic, with holocrystalline ophitic ground mass with olivine, andesitic labradorite and augite. Andesine is common in the intermediate rocks. K-Ar ages of 2.5 and 2.8 Ma were reported from these basalts, with possible lower age 3.5 Ma and upper 1.5 Ma (Kazmin etal, 1980). According to Tsegaye et al. (2005) the dominant lava flows in the area north of the basin are represented by plagioclase-phyric basalts with minor fine grained and scoracious varieties. Few olivine and pyroxene-phyric lava flows are reported. The basalts are generally quartz tholeiites with few olivine basalts. The exposed thickness varies form few to about 30m along fault escarpments.

4.1.6 Stratoid silicics: ignimbrites unwelded tuff, ash flows, rhyolites (N1-2n)

In the study area lithologies of stratoid silicics, ignimbrites, unwelded tuffs, ash flows, rhyolites and trachytes (N1-2n) constitute a considerable portion of the rift escarpments especially in the western part near Munesa town, while in the floor they are unconformably overlapped by younger volcanic of the Dino formation. The time of formation of the Nazreth group is between 9.5 and 3 Ma years (Kazmin and Seife M., 1978). Wolde Gabriel et al., (1990) reported a thickness of more than 600 m for the Pliocene pyroclastic units in the eastern margin of the rift in the Munesa area.

4.1.7 Nazret Group and Dino Formation undifferentiated (NQs)

The silicic rocks of the Dino Formation are not only confined to the rift floor but are extensively developed in escarpments and on the adjacent plateau where they could not be separated from the silicics of the Nazret Group, they were mapped as Nazret Group and Dino Formation undifferentiated (NQs). In the rift escarpments where 500 meters and more of silicic rocks is locally exposed: both units are almost certainly present but in most cases the data is not sufficient to separate them. It was noted that on both sides of the rift the upper part of the section normally bears evidence of lacustrine sedimentation in the form of bedded water lain tuffs, sediments, etc. This bedded sequence correlates well lithologically with young (Pleistocene) rift floor silicic and is most probably of the same age.

4.1.8 Lacustrine Sediments, silts, clays, diatomites (Ql)

In the rift Quaternary sediments and mostly lacustrine origin are intercalated with Pliocene to Pleistocene ignimbrites both in the rift floor and rift shoulders. The older sediments are lacustrine diatomites, tuffaceous clays and silts interbedded with basal ignimbrites of the Nazreth Group.

The lacustrine sediments are intercalated with redeposited volcanic ash and tuffs. The lacustrine sediments are mainly represented by sand and silt. The major components of the sediments are volcanic origin, such as pumice and volcanic ash, obsidian, rhyolite and basaltic rock fragments (Tsegaye et al., 2005; Bevenuti et al., 2002).

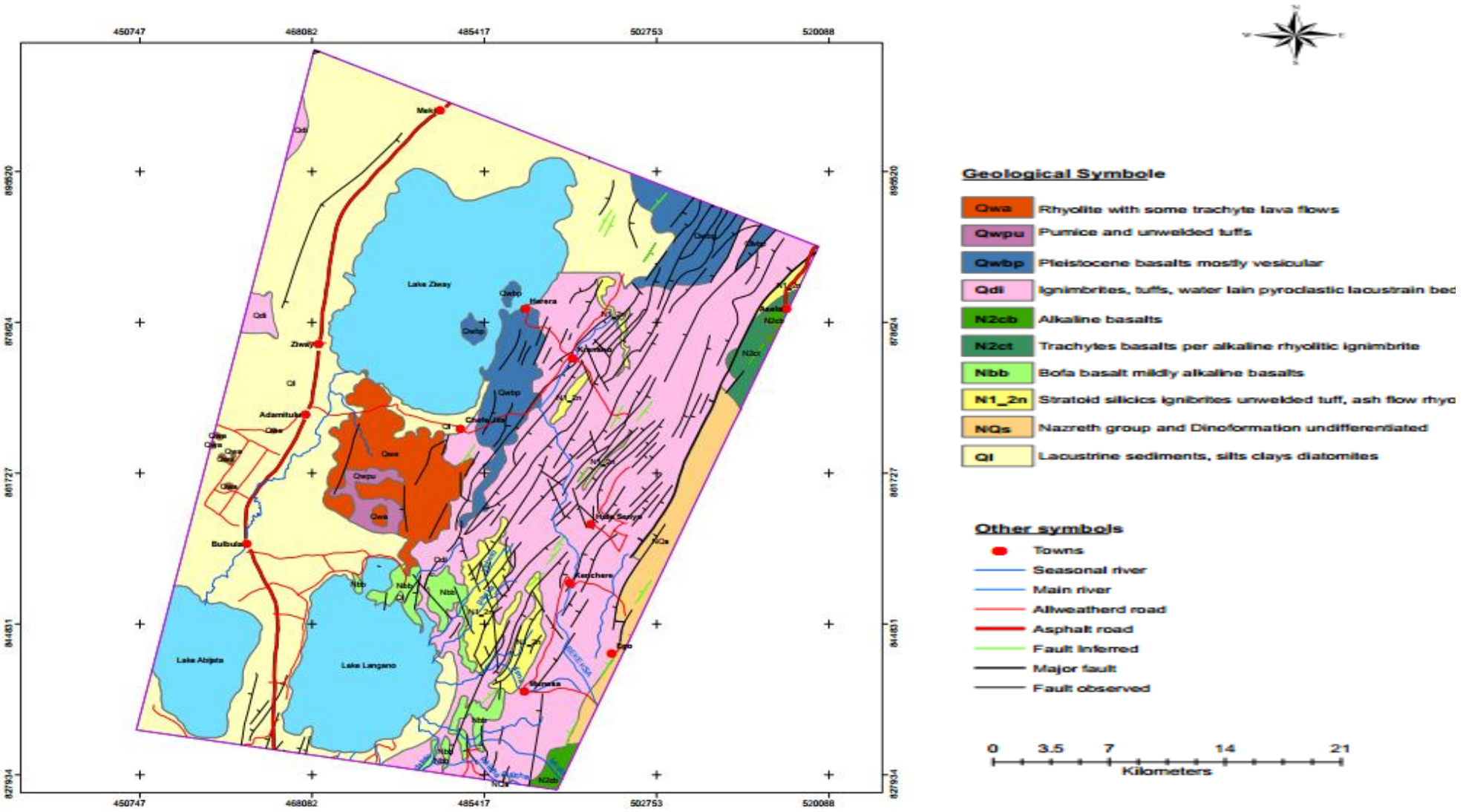

Fig. 4.1 Geological map of the study area (modified from geological map sheet of Geological Survey, Ethiopia (2004))

4.2 STRUCTURAL DESCRIPTION OF THE STUDY AREA

Structural map of the study area Fig (4.4) shows different structural features that were observed and mapped during and after the field survey. The major structural features are faults and fractures and are described as follows:

4.2.1 Faults: are brittle fractures along which measurable displacement has occurred. Brittle deformation results in the breaking of rocks. It normally occurs in rocks that are near the surface of the Earth and therefore in an environment of low confining pressure, or in rocks that are naturally strong and which therefore are less likely to bend. Rocks that are prone to brittle deformation break when subjected to stress. When rocks break, one of 3 things can occur: 1) cracking/fracturing 2) jointing 3) faulting: Faulting occurs when there is movement along the plane of breakage induced by brittle deformation.

The geological structures observed in the study area are part of the brittle deformation and they are oriented almost similar to the orientation of the central MER, i.e. NE direction. These are some orthogonal to the rift axis faults occur in the Langano area forming the pull-apart basin (Bocalleti et al. 1998). The study area is part of the central sector of the MER mainly part of the eastern margin and characterized by well-defined boundary faults of assela – Langano fault system and internal wonji fault belt segments.

The northeastern corner of the Lake Langano lies within the Haroresa Rhomboid Fault System, which has resulted from the intersection between two fault trends: a dominant NNE to NE-trending fault set, and a minor N-to-NNW-trending fault set. These fault systems gave rise to horst, graben and half-graben structures mainly trending around NNE to NE. On the eastern part of Ziway Lake up to Asela there are different field observation are made. The structural measurements that are associated with a good kinematic indicators are mainly carried on steeply dipping normal faults. Most of structural field measurements are carried out along Faults associated near Katar River, Ogolcho, faults along the road side of Thure and the Golja fault. Almost all faults with the associated kinematic indicators are measured along the fault Plane are striking from NNE- SSW, NE- SW, ENE- WSW and NNW – SSE direction.

The study area are characterized by very impressive fault escarpments. The fault planes record evident striations that allowed the measurements of a number of good quality fault-slip data. Thus

all the measurements of silken lines or striations taken along the fault plane are very helpful to analyze the present kinematics of the eastern margin of the central main Ethiopian rift.

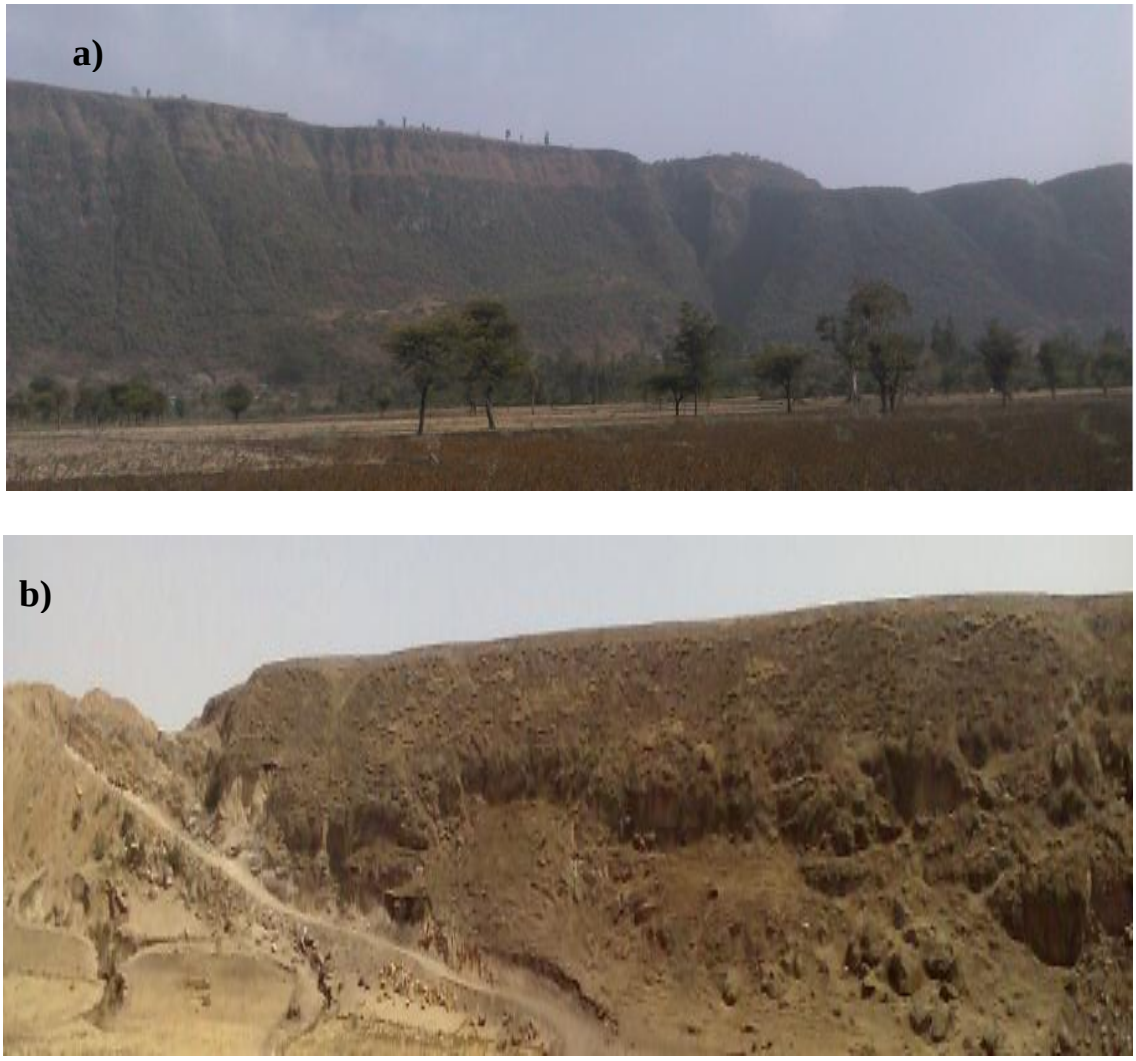

Fig. 4.2 Photographs showing major faults a) Asela fault b) Golja fault along the quarry site

4.2.2 Fracture: faults are another form of fracture. Fractures are forms of brittle deformation that are the result from shear or tensile stress. On the study area on the way of Thure village with a location 08^{o}03.582' and 039 06. 915; elevation of 1857 m there are faults that are with associated fractures. Tilting of major fault due to associated fractures results small horst graben structures. This tensional fractures may be related with later deformation activity which affect the fault of the area.

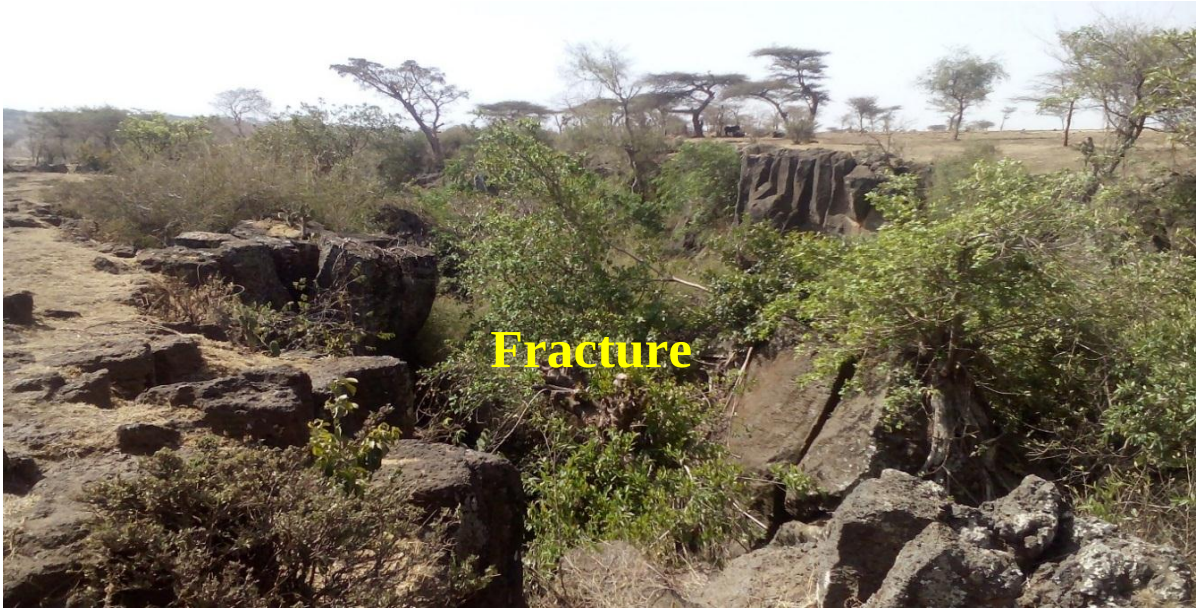

Fig. 4.3 Fracture

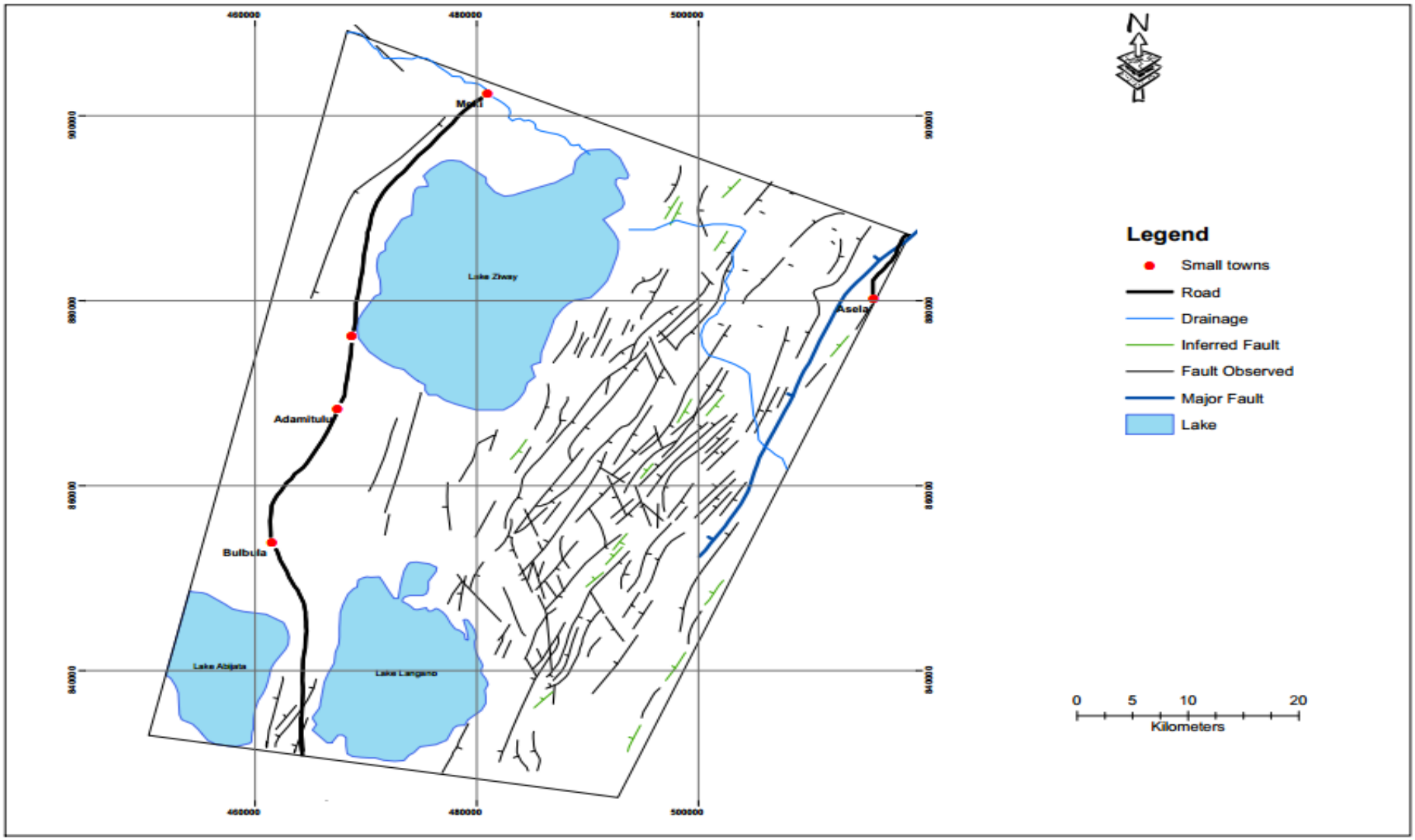

Fig. 4.4 Structural map of the study area: fault strikes and dip directions are digitized from Google Earth image

CHAPTER FIVE

5. KINEMATIC ANALYSIS OF FIELD DATA

5.1 KINEMATIC ANALYSIS

To constrain the stresses driving slip on faults in the eastern margin of the central main Ethiopian rift; kinematic analysis performed by using faultkin structural software to determine the principal stress axis. Kinematic analysis was carried out using so-called 'faultkin analysis' techniques. The analysis of fault slip data yields information concerning the orientation of the strain to compute σ1 compression and extension σ3 extension direction.

The present day stress regime was determined from focal mechanisms of earthquakes that have occurred in the study area. The aims of the study here were: 1) to determine the fault movements 2) to derive a fault plane solution from the field data and a fault pattern to compare it with the regional fault pattern from fault kin analysis technique 3) to drive extension direction.

Faults associated slip-striations have been measured at over 13 fault blocks across the eastern margin of central main Ethiopian rift. In total twenty eight (28) faults with good kinematic indicators were recorded. More than 80% of the faults measured exhibit good kinematic indicators, (striation).

Almost all exposures in the mapping area were welded ignimbrites and there are also pyroclastic material and some alluvial deposit are there. These rocks exhibit N-S to NNE to SSW trending striations. Fault exposures varied from large faults in a relatively undeformed country rock, to fault zones of fractured rock. Most of the striations are observed on brecciated fault rock this is because of this rock types are easily susceptible to deform and brecciate than that of ignimbrite rock which is dominant at the area.


a

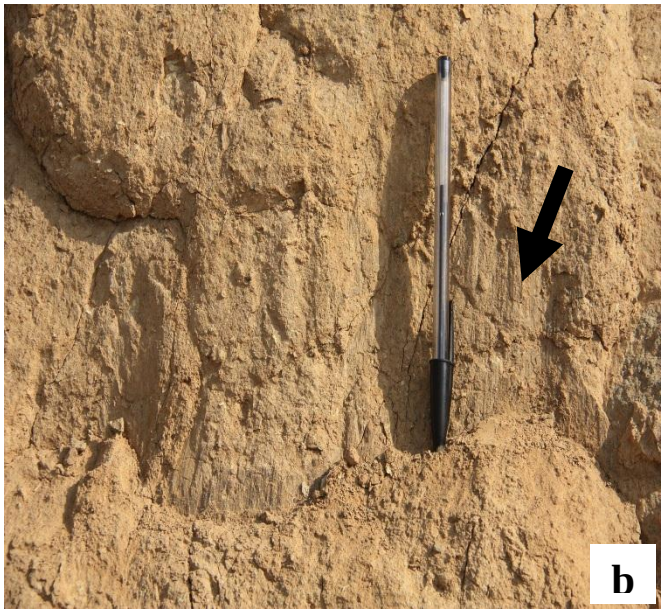
b

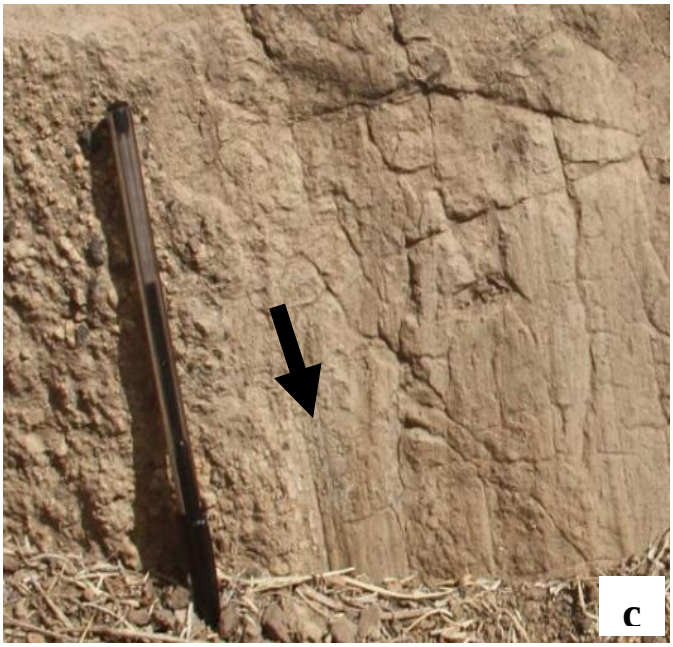
c


d

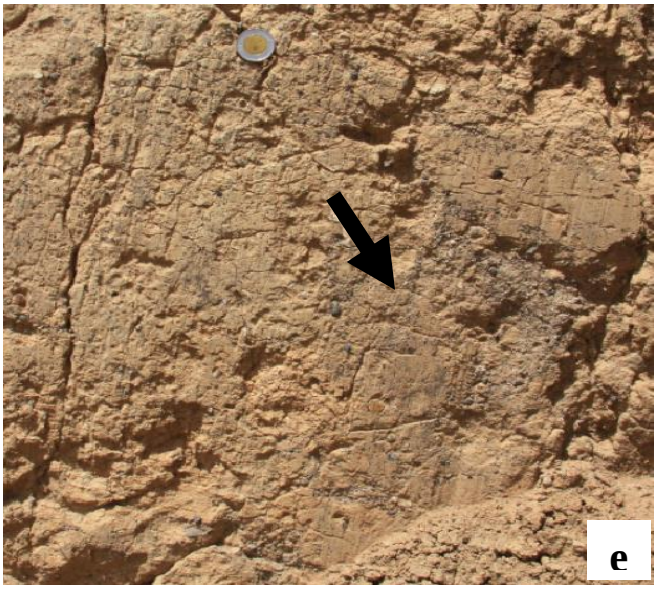
e

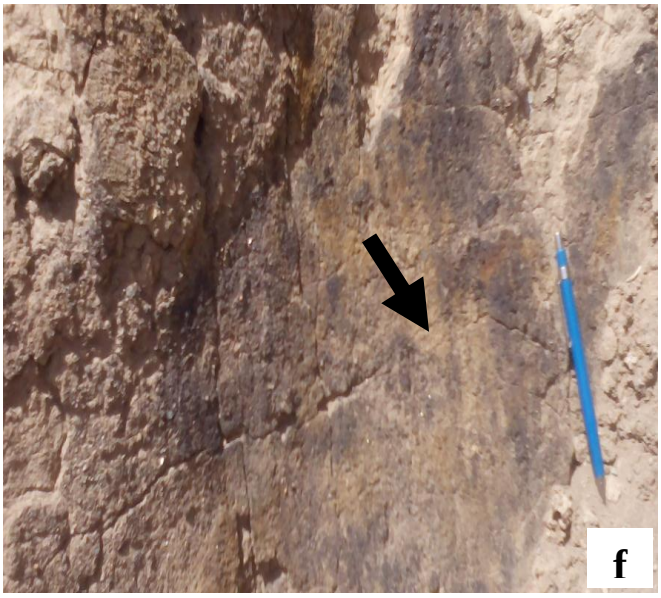
f


g

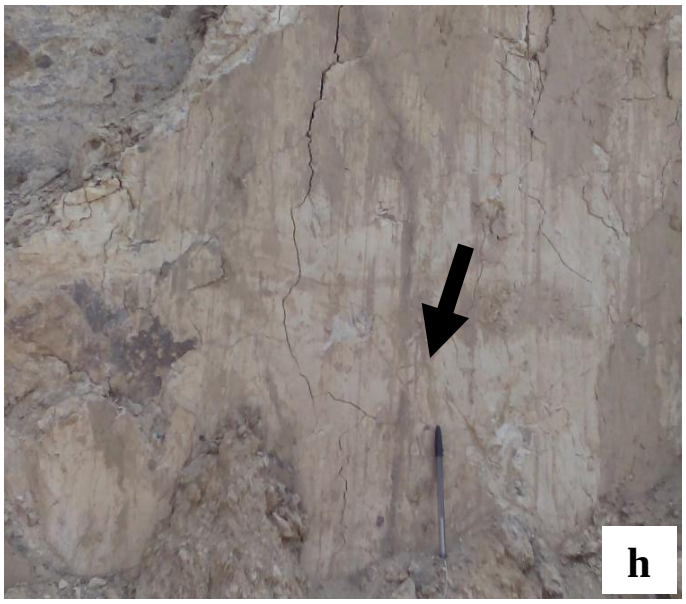
h

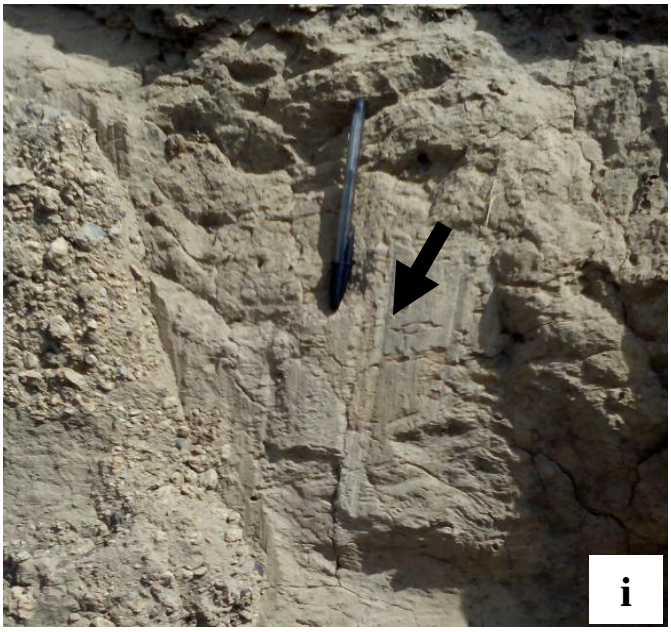
i


j


k


l

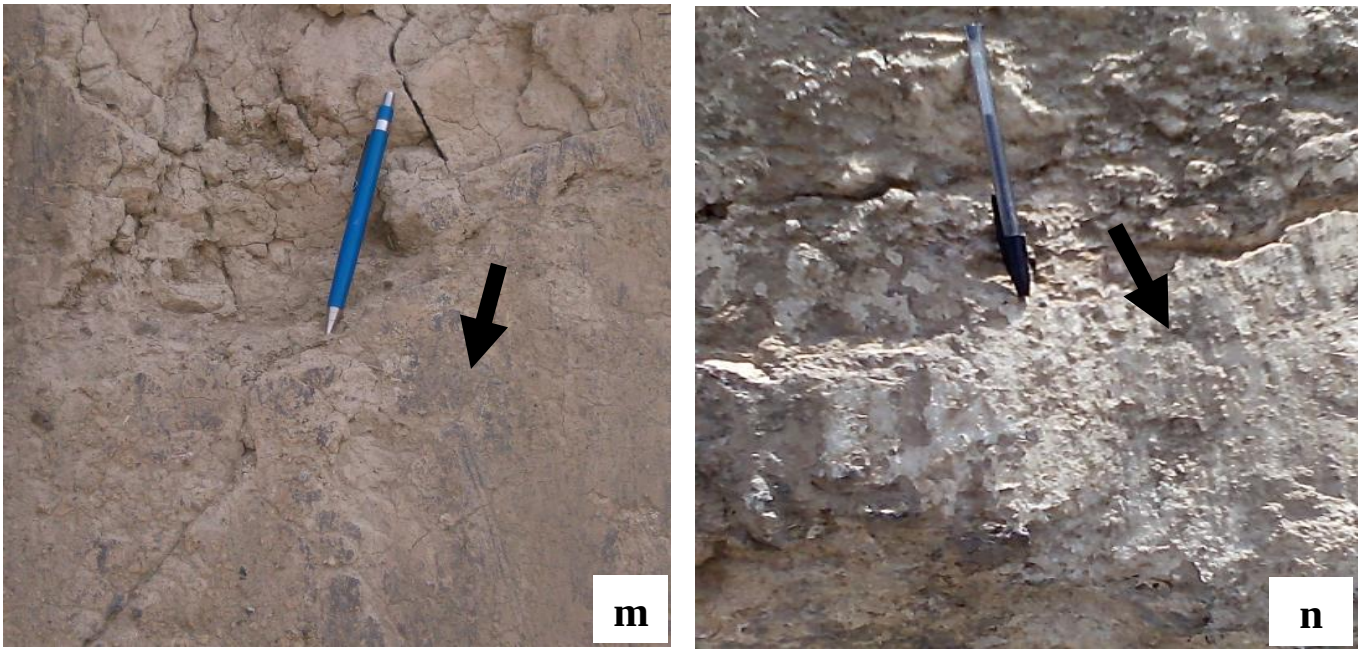

Fig. 5.1 Striations (grooves) on rock surface from which a measurement taken

On Figure 5.1 above from (a-n) all are representing the kinematic indicators: the arrow on all photographs are used to show those striations. On all the photographs this striations or grooves are oriented nearly N to S directions. Photographs of **a, b, c, g** and **h** are taken from the Golja major fault along which different measurements are taken with the associated striations (grooves). The orientations of this major fault are striking from NE to SW and NNE to SSW direction. Photograph **a:** ignimbrite, **b:** fault breccia in which they found at the foot of the fault surface of this Golja major fault **c:** tuff **g:** poorely welded ignimbrites and **h:** tuff; these photographs are belonging to the structural data listed on table 5.5 from s.no 11-19. Photographs of **e, j, k** and **m** are also taken from the other side of the Golja major fault. **e:** ignimbrite, **j:** tuff; on which striations are visible along the fault plane, **k:**tuff which is weathered and the striations are covered by weathering activity but it is possible to see the grooves on the rock after removing covering weathered material easily from a rock, **m:** ignimbrite. The orientation of the faults NE to SW and from NNE TO SSW direction. This photographs are matched with some of the structural data of table 5.1 from s.no 20-28. Photographs of **d** and **f a**re taken from the fault near the Katar River on the ignimbrite outcrop. The fault plane is oriented nearly to the N-S direction. The scratches of striations are seen the rock. This photographs of information are correlated with the table 5.1 from s. no 2-4. Photos of **i, l** and **n** are taken from

the faults near the Asela major fault. All three photographs are ignimbrites and the fault is oriented nearly N-S direction. This data is matched with s. no 2 and 6 of table 5.1.

5.2 RESULTS OF FAULT KINEMATIC ANALYSIS AND DISCUSSION

The results of the structural and kinematic analysis carried out in the eastern margin of central main Ethiopian rift from Langano, Ziway up to Assela area allowed us to define the geometry of faults, kinematics and extension direction from both field work and satellite image interpretation acting on the study area. The actual nature and trend of fault structures as well as the exact geometry and the present day stress state can be derived from kinematic analysis of faults observed and measured at the study area.

The kinematic analysis technique for fault-kinematics data, proposed by Richard W. Allmendinger (2012) used to compute the directions of compression ($\sigma 1$) and extension ($\sigma 3$). For this, fault planes along which significant movement easily visible at the outcrop scale has been used.

There are steps for sorting the fault data in the present study by using Fault kin structural software. The first step is entering the raw structural data collected from field. Next the software calculates all the required output from the entered raw data. Finally based on the several options on the plot tab the software demonstrates result for the input data.

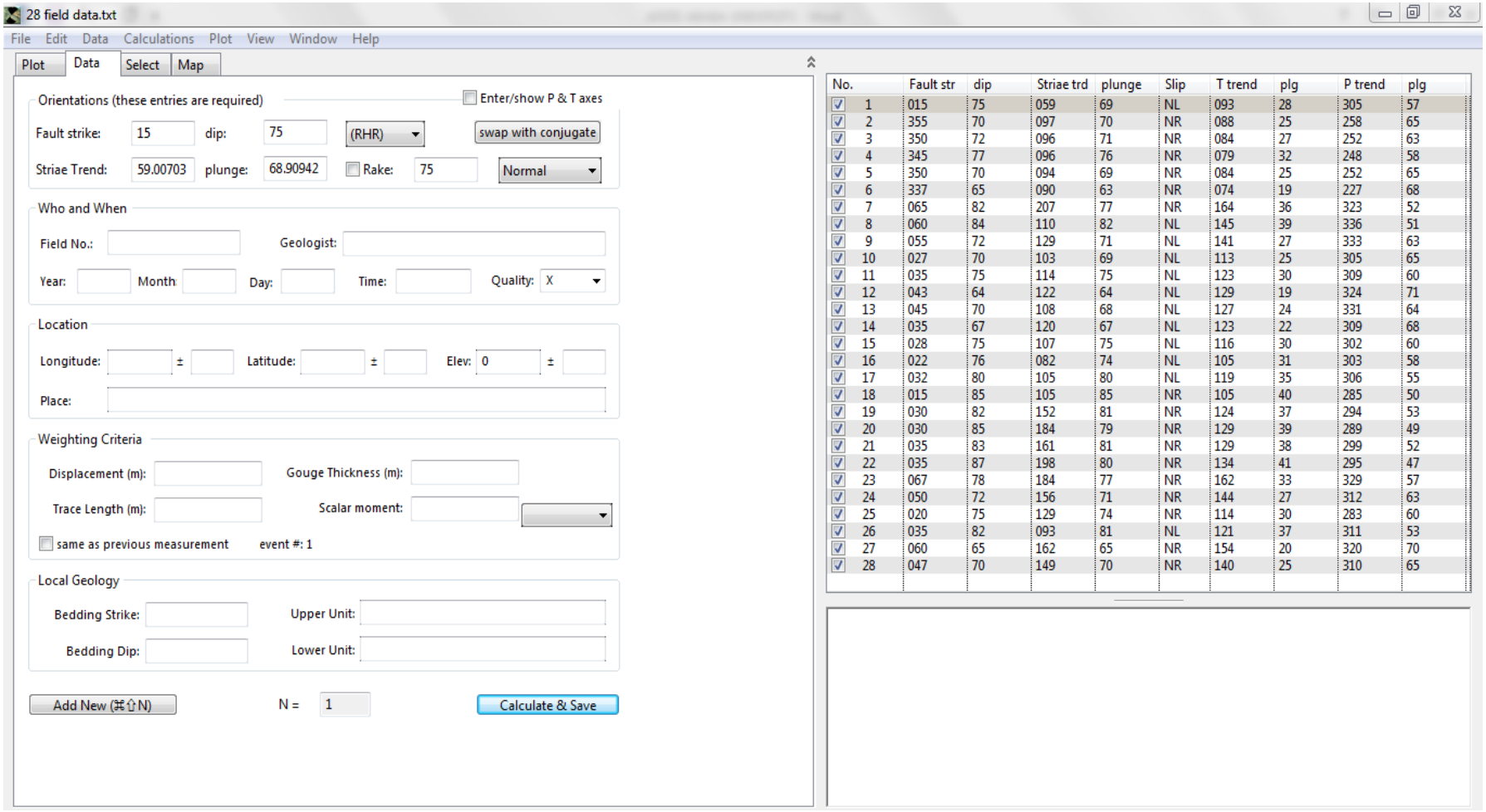

Fig. 5.2 Out puts calculated by the Faultkin software for 28 fault slip data

Table 5.1 Results from kinematic analysis of field data

S.No	Fault strike	Dip	Striae trend	Plunge	Slip	T trend	Plunge	**P** trend	Plunge
1	015	75	059	69	NL	093	28	305	57
2	355	70	097	70	NR	088	25	258	65
3	350	72	096	71	NR	084	27	252	63
4	345	77	096	76	NR	079	32	248	58
5	350	70	094	69	NR	084	25	252	65
6	337	65	090	63	NR	074	19	227	68
7	065	82	207	77	NR	164	36	323	52
8	060	84	110	82	NL	145	39	336	51
9	055	72	129	71	NL	141	27	333	63
10	027	70	103	69	NL	113	25	305	65
11	035	75	114	75	NL	123	30	309	60
12	043	64	122	64	NL	129	19	324	71
13	045	70	108	68	NL	127	24	331	64
14	035	67	120	67	NL	123	22	309	68
15	028	75	107	75	NL	116	30	302	60
16	022	76	082	74	NL	105	31	303	58
17	032	80	105	80	NL	119	35	306	55
18	015	85	105	85	NR	105	40	285	50
19	030	82	152	81	NR	124	37	294	53
20	030	85	184	79	NR	129	39	289	49
21	035	83	161	81	NR	129	38	299	52
22	035	87	198	80	NR	134	41	295	47
23	067	78	184	77	NR	162	33	329	57
24	050	72	156	71	NR	144	27	312	63
25	020	75	129	74	NR	114	30	283	60
26	035	82	093	81	NL	121	37	311	53
27	060	65	162	65	NR	154	20	320	70
28	047	70	149	70	NR	140	25	310	65

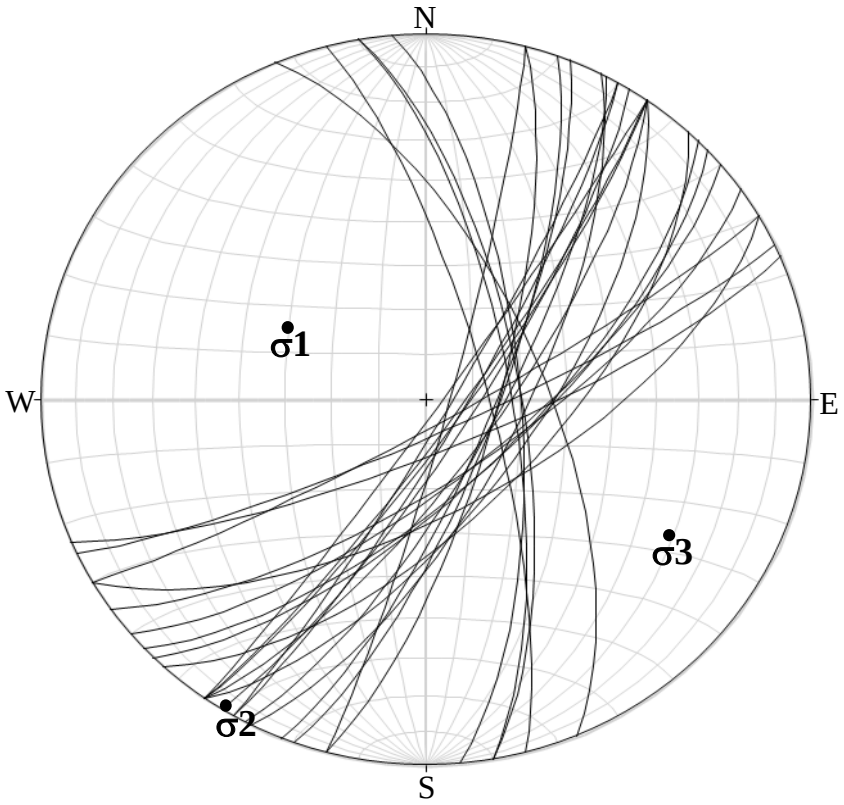

Fig. 5.3 Twenty eight fault planes σ1, σ2, σ3 of kinematic axis

The methodology of fault-kinematics analysis to determine stress fields along the eastern margin has been applied in a number of tectonically active regions. The present-day stress regime was determined from the focal mechanisms of earthquakes that have occurred in the area. Field observations of kinematic indicators from different segments of the eastern margin of the central main Ethiopian rift indicate that the fault kinematics was predominantly normal fault.

When plotted stereographically from Fig. 5.3, four main fault clusters are apparent, with strike orientations that closely match the data derived from kinematic analysis. These clusters reflect have four distinct fault geometries: 1) NNE–SSW trending faults 2) NNW–SSE trending faults 3) ENE-WSW trending faults and 4) NE-SW trending fault. These four fault geometries are dipping to NE direction.

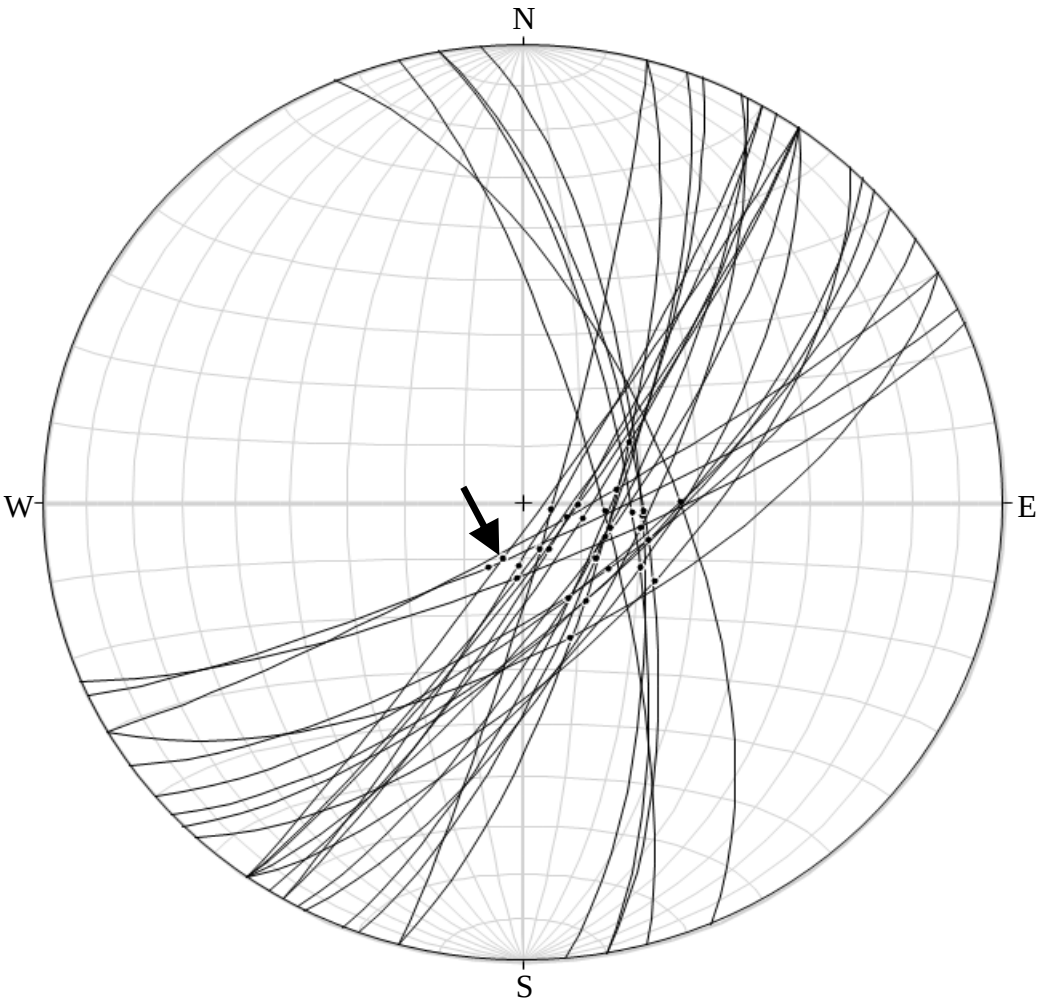

Fig. 5.4 Striations along with the fault planes the arrow indicates the striations represented by black dots.

Field observations suggest that many of the faults of outcrop dip at an average of ~75º. Fault kinematic analysis suggests the existence of different fault geometries at the eastern margin of central main Ethiopian rift: this difference in fault geometries may be related either to temporal or spatial variation in deformation. The study area has an impressive normal faults that show extensional features indicated by kinematic analysis of focal mechanisms of earthquake solution.

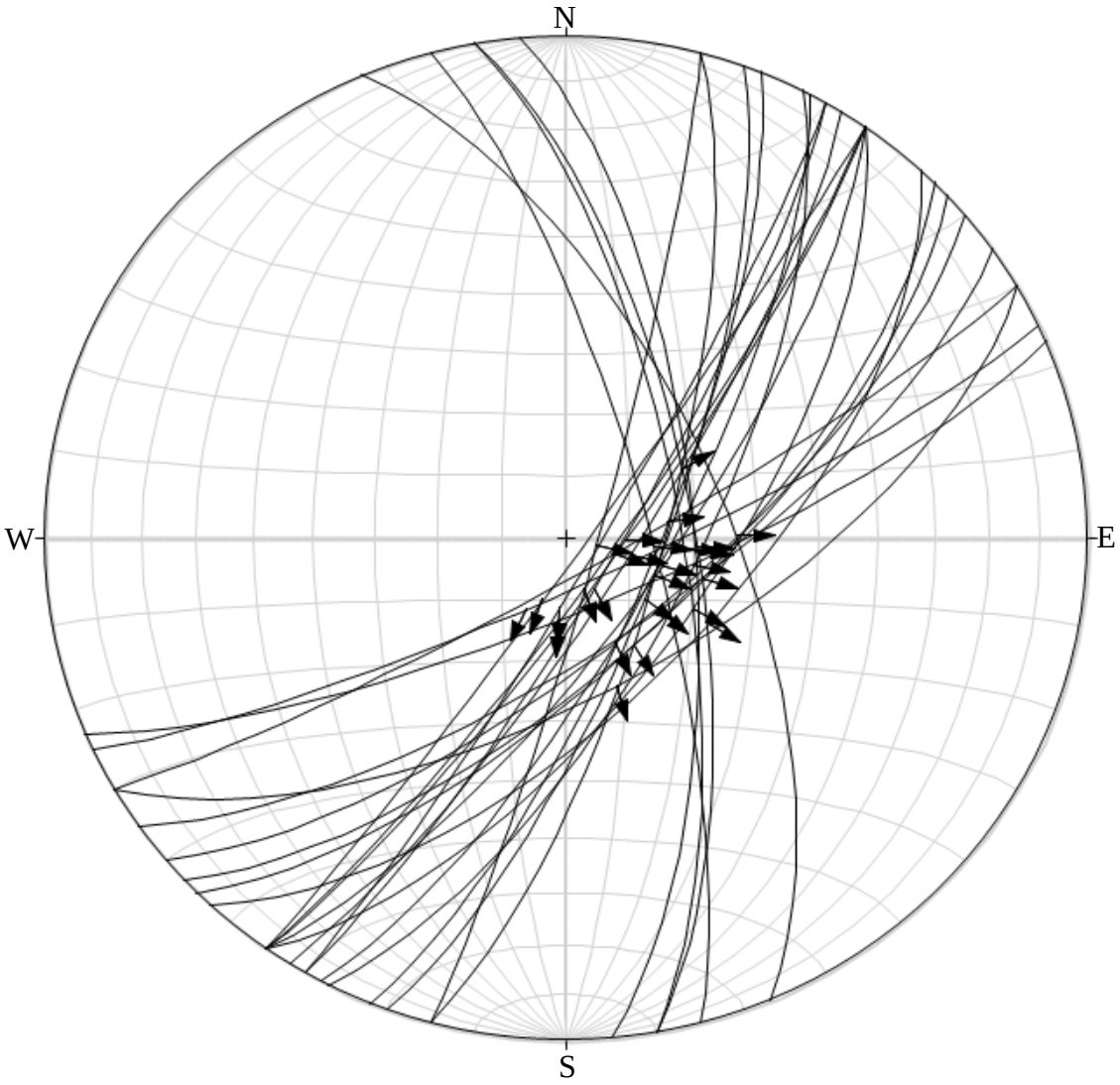

Fig. 5.5 Fault plane showing hanging wall slip direction for 28 measurements from field

From the kinematic analysis of those faults, we obtained a focal mechanism fault plane solution showing a high angle normal fault. From the analysis of the fault data maximum compressive stress σ1=300/60 intermediate compressive stress σ2= 210/00 and minimum horizontal compressive stress σ3= 120/30.

The results based on the kinematic analysis measured on fault planes of various scales in which tectonic effect commonly expressed on ignimbrite outcrops as well as on some fault breccia's , yield a high angle normal.

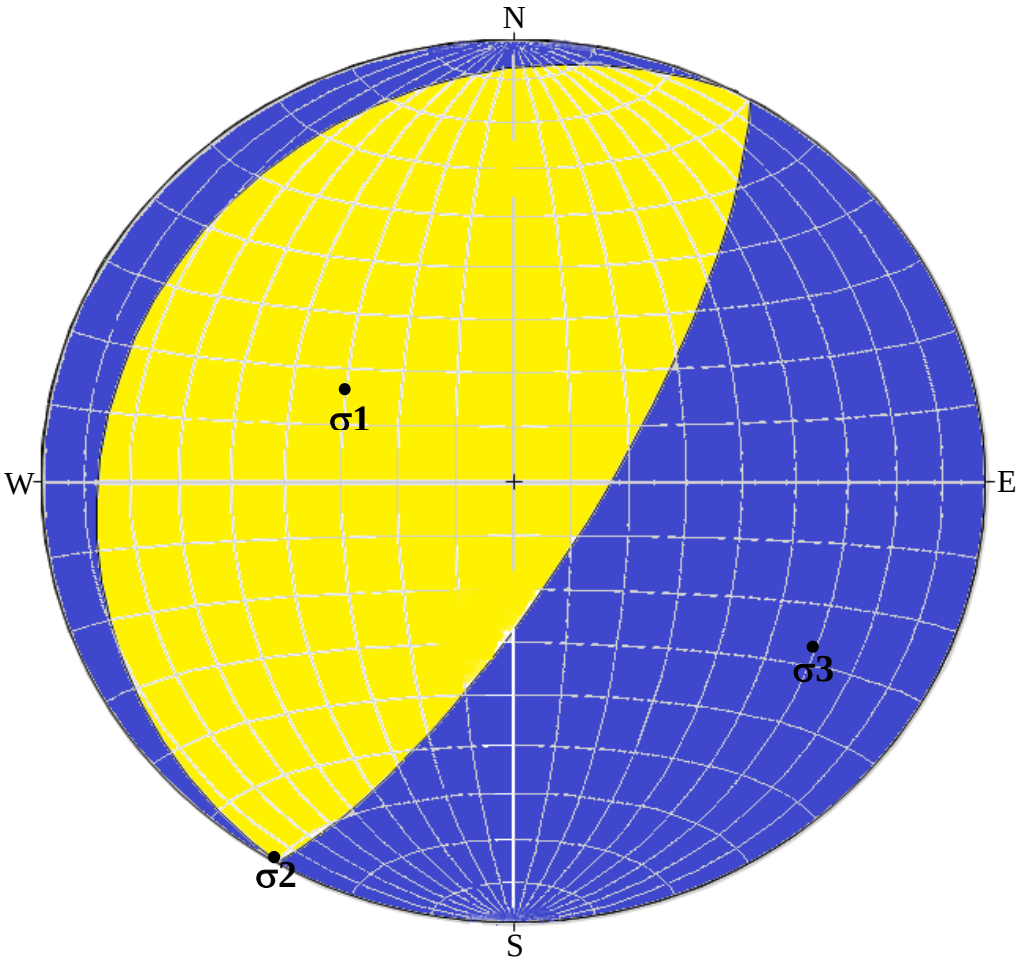

Fig. 5.6 Focal mechanism solution for 28 field data showing the three kinematic axis σ1, σ2 and σ3

Understanding of regional and local fault population measured at outcrop scale that exhibit measurable fault surface orientation and kinematic indicators such as slicken line data sets and when combined with focal mechanism solution of the present day stress state better characterize that the deformation on the area is as a result of extension.

Detailed morphological and field analyses have been made in the eastern margin of central main Ethiopian rift. In this part of the rift, major fault scarps have been identified and measured on the field. We gather the information on main fault direction and considering the marginal faults of Asela and Langano and the internal active faults around Ogolcho and Katar River.

The study of earthquake focal mechanisms allows us to view the geometry and orientations of faults at the time of movement. Combining the focal mechanism data with the longer term geological record, it is possible to reconstruct the tectonic process of a region through time. In this study the focal mechanism solution result from twenty eight measurements of faults with striations at the eastern margin are considered as a consequence of the 1906 Langano earthquake.

Most of the data collected at the eastern margin are taken from the golja fault and faults near Katar River and it is quite clear that in both areas of the study the normal fault dominate. Based on structural analysis in the eastern margin; extension seems to be a common form of deformation.

5.3 INVERSION OF FOCAL MECHANISM

The inversion of fault slip data along the central main Ethiopian rift from (Agostini et al., 2011) involves the distribution of faulting that has to be investigated along three distinct transects crossing the rift from the western margin (Guraghe margin) to the eastern rift margin (Asela margin). Inversion of fault slip data along the central main Ethiopian rift is given in table 5.2 below. Kinematic indicators on fault planes were measured in order to establish the mean slip vector. Data have been elaborated by using the right dihedron inversion method to determine the stress tensors [Angelier and Mechler, 1977; Angelier, 1979]. The database consists of 47 sites of measurements and the obtained stress axis orientations are reported in Table 5.2.

Table 5.2: Inversion of fault slip data of central main Ethiopian rift (Agostini et al., 2011)

Station	Number of Data	Lat	Long	Age of Youngest Deformed Rock	σ1		σ2		σ3	
					Dip Dir.	Dip	Dip Dir.	Dip	Dip Dir.	Dip
1	8	8°58′52.54″N	39°47′11.39″E	Quaternary	117	58	26	0	*296*	*32*
2	4	8°33′13.22″N	39°18′16.16″E	Pliocene	316	60	170	25	*74*	*15*
3[b]	10	8°30′05.09″N	39°10′54.08″E	Quaternary	318	85	181	6	*90*	*5*
4[b]	7	8°23′24.11″N	39°12′00.00″E	Late Quaternary	278	56	187	1	*96*	*34*
5	10	8°17′08.65″N	39°25′46.99″E	Quaternary	186	80	9	10	*279*	*10*
6	10	8°17′00.70″N	39°29′00.53″E	Holocene (5 ka)	178	65	56	14	*320*	*20*
7	2	8°15′31.82″N	39°30′07.77″E	Quaternary	83	55	249	35	*344*	*6*
8	7	8°17′27.59″N	39°30′39.81″E	Pliocene	83	69	236	19	*329*	*9*
9	5	8°15′37.54″N	39°10′10.68″E	Quaternary	119	62	10	10	*275*	*26*
10	3	8°15′24.86″N	39°11′15.32″E	Quaternary	183	11	67	66	*277*	*21*
11[b]	10	8°16′17.03″N	38°29′31.11″E	Quaternary	1	86	230	2	*140*	*3*
12	3	8°05′15.19″N	38°58′41.71″E	Late Quaternary	180	17	62	56	*280*	*28*
13	6	8°04′12.75″N	39°08′24.20″E	Quaternary	172	34	48	40	*286*	*32*
14	5	8°00′59.85″N	39°05′23.40″E	Pliocene	53	3	308	78	*144*	*11*
15	3	8°00′35.80″N	39°03′06.96″E	Quaternary	88	54	237	32	*337*	*15*
16	8	8°00′24.55″N	39°05′49.49″E	Quaternary	102	74	244	13	*336*	*10*
17	8	8°05′00.38″N	38°10′54.05″E	Pliocene	273	55	20	12	*118*	*33*
18[b]	7	8°03′30.02″N	38°16′48.06″E	Pliocene	65	80	196	6	*287*	*7*
19	6	8°00′23.92″N	38°21′25.71″E	Quaternary	295	59	204	1	*114*	*31*
20	4	7°57′50.56″N	38°16′32.67″E	Late Quaternary (39–30 ka)	316	66	200	11	*105*	*21*
21	4	7°55′24.31″N	38°56′02.64″E	Late Quaternary	331	51	225	13	*124*	*36*
22	20	7°52′47.84″N	38°57′15.30″E	Late Quaternary	303	60	213	0	*123*	*30*
23	8	7°52′38.98″N	38°55′28.45″E	Quaternary	323	56	220	8	*124*	*32*
24	6	7°50′55.47″N	38°51′43.86″E	Quaternary	340	51	208	29	*104*	*24*
25	22	7°50′40.64″N	39°00′14.34″E	Late Quaternary	58	63	195	20	*291*	*17*
26	3	7°52′44.53″N	38°08′24.10″E	Pliocene	293	60	198	3	*106*	*30*
27	4	7°52′04.46″N	38°10′14.30″E	Quaternary	19	78	246	8	*154*	*8*
28	4	7°45′17.71″N	38°54′32.85″E	Pliocene	55	68	179	13	*273*	*17*
29	4	7°43′51.08″N	38°55′17.03″E	Quaternary	132	58	26	10	*291*	*30*
30	3	7°43′08.23″N	38°55′28.96″E	Holocene (9 ka)	101	59	239	24	*337*	*18*
31	6	7°41′48.85″N	38°49′48.50″E	Quaternary	48	82	243	7	*152*	*2*
32	12	7°40′22.94″N	38°48′37.87″E	Holocene (8–7 ka)	243	73	357	7	*89*	*16*
33	6	7°38′44.42″N	38°54′26.87″E	Pliocene	194	70	359	19	*90*	*5*
34	16	7°40′20.68″N	37°59′46.80″E	Pliocene	350	62	167	28	*258*	*1*
35	20	7°37′26.68″N	37°55′27.59″E	Holocene (1 ka?)	286	67	39	10	*133*	*21*
36	7	7°36′05.53″N	38°04′53.19″E	Quaternary	88	62	340	9	*245*	*26*
37	6	7°32′48.09″N	38°54′26.76″E	Quaternary	13	73	204	16	*113*	*3*
38	5	7°32′48.70″N	38°54′28.01″E	Quaternary	10	80	192	10	*102*	*0*
39	6	7°30′55.75″N	38°48′33.12″E	Pliocene	28	52	191	36	*287*	*8*
40	8	7°28′30.81″N	38°45′03.80″E	Pliocene	233	74	37	15	*129*	*4*
41	3	7°27′00.04″N	38°50′10.80″E	Pliocene	109	58	248	25	*346*	*18*
42	8	7°16′50.41″N	38°30′06.90″E	Quaternary	118	60	11	10	*276*	*28*
43	12	7°05′42.57″N	38°45′29.95″E	Pliocene	214	64	120	2	*29*	*30*
44	11	6°27′42.37″N	37°44′24.20″E	Quaternary	277	68	22	6	*115*	*22*
45[b]	7	6°10′36.00″N	37°34′43.10″E	Oligocene	25	87	167	2	*251*	*3*
46[b]	13	6°07′21.09″N	37°37′32.93″E	Quaternary	159	86	46	1	*315*	*3*
47[b]	7	5°59′32.08″N	37°32′16.03″E	Quaternary	190	66	353	23	*86*	*6*

In the central MER the obtained extension directions show complex patterns, with significant variations passing from the rift margins to the WFB system. Cumulative analysis of fault slip data performed for the various MER sectors, support differences in paleostress orientation along border faults and in-rift WFB faults. These elaborations suggest an overall N90°–110°E extension across the MER , which fits, within errors, the current Nubia-Somalia relative motion based on the analysis of geodetic data [e.g., Bilham et al., 1999; Fernandes et al., 2004; Bendick et al., 2006;Stamps et al., 2008].

Table 5.3: Earthquake Source Parameters Determined From EAGLE (Kier et al., 2006)

Event	Date, year/month/day	Time, UT	Latitude, °N	Longitude, °E	Depth, km	Strike	Dip	Rake	M_L
1	2002/01/16	2122:39.44	9.239	40.021	13.25	180.00	50.00	−90.00	1.7
2	2002/01/17	0138:03.91	8.154	39.002	20.29	2.27	60.05	−93.46	2.01
3	2002/01/18	0142:40.83	8.998	39.918	10.23	359.67	54.23	−97.40	2.82
4	2002/02/17	0238:15.44	9.470	39.692	11.86	171.52	66.00	−90.00	3.21
5	2002/05/02	2143:23.17	9.122	39.984	13.16	211.58	56.38	−80.38	2.64
6	2002/07/04	0259:42.35	9.173	39.966	15.84	214.40	60.08	−85.38	3.54
7	2002/07/31	0154:38.27	9.444	39.677	11.25	172.76	66.06	−85.62	2.34
8	2002/08/21	0127:23.93	8.951	39.711	13.85	192.88	60.13	−84.23	2.14
9	2002/10/08	1937:43.42	9.199	39.949	12.65	225.74	68.06	−85.69	2.03
10	2002/10/09	1819:37.91	9.193	39.987	12.52	223.13	68.19	−64.02	2.14
11	2002/10/10	1915:51.93	9.066	39.965	14.59	201.49	58.30	−66.30	1.17
12	2002/10/19	2125:25.96	10.130	39.957	15.47	198.07	59.38	−71.32	2.83
13	2002/11/04	0017:42.49	8.432	39.673	12.91	2.54	51.18	−83.58	1.17
14	2002/11/04	0024:55.49	7.812	38.976	6.88	183.82	63.32	−109.10	1.71
15	2002/11/05	2242:14.69	9.728	39.370	14.65	29.29	66.39	−79.08	1.92
16	2002/11/07	0124:31.21	9.492	40.040	15.48	216.30	46.04	−74.63	1.89
17	2002/12/03	1602:52.26	7.481	38.553	13.63	183.71	68.01	−92.16	2.55
18	2002/12/03	2010:01.33	7.700	38.911	12.43	190.00	45.00	−90.00	2.34
19	2002/12/04	1341:09.57	8.873	39.836	9.57	209.92	60.00	−90.00	1.97
20	2002/12/13	1736:21.66	9.494	40.034	15.79	183.69	64.27	−98.89	2.2
21	2002/12/15	0837:35.26	7.428	38.648	8.61	197.95	50.00	−90.00	3.06
22	2002/12/15	1915:38.82	7.430	38.657	6.42	210.49	70.38	−78.31	2.89
23	2002/12/15	2035:05.22	9.548	40.144	19.01	190.55	66.56	−103.10	1.93
24	2002/12/17	2212:36.10	9.001	39.907	8.44	64.49	88.17	−0.81	1.4
25	2002/12/17	2315:10.76	8.998	39.901	9.17	71.95	80.73	−3.78	1.55
26	2002/12/23	0627:49.95	9.446	39.680	10.43	181.99	60.00	−90.00	2.45
27	2002/12/26	1947:51.98	9.221	40.014	12.96	213.15	62.02	−87.74	3.17
28	2002/12/26	1955:17.90	9.221	40.011	12.65	219.89	60.00	−90.00	2.41
29	2003/01/02	0852:45.37	9.246	40.013	13.91	195.00	65.00	−90.00	2.37
30	2003/01/10	1213:56.08	8.611	39.447	7.00	42.64	85.25	13.19	3.44
31	2003/01/13	2106:00.76	9.491	39.681	11.17	168.45	56.21	−97.23	1.97
32	2003/01/20	2116:22.90	7.475	38.823	11.74	206.12	42.96	−104.76	2.52
33	2003/01/21	0808:18.85	7.495	38.822	11.41	197.78	37.16	−117.15	2.9

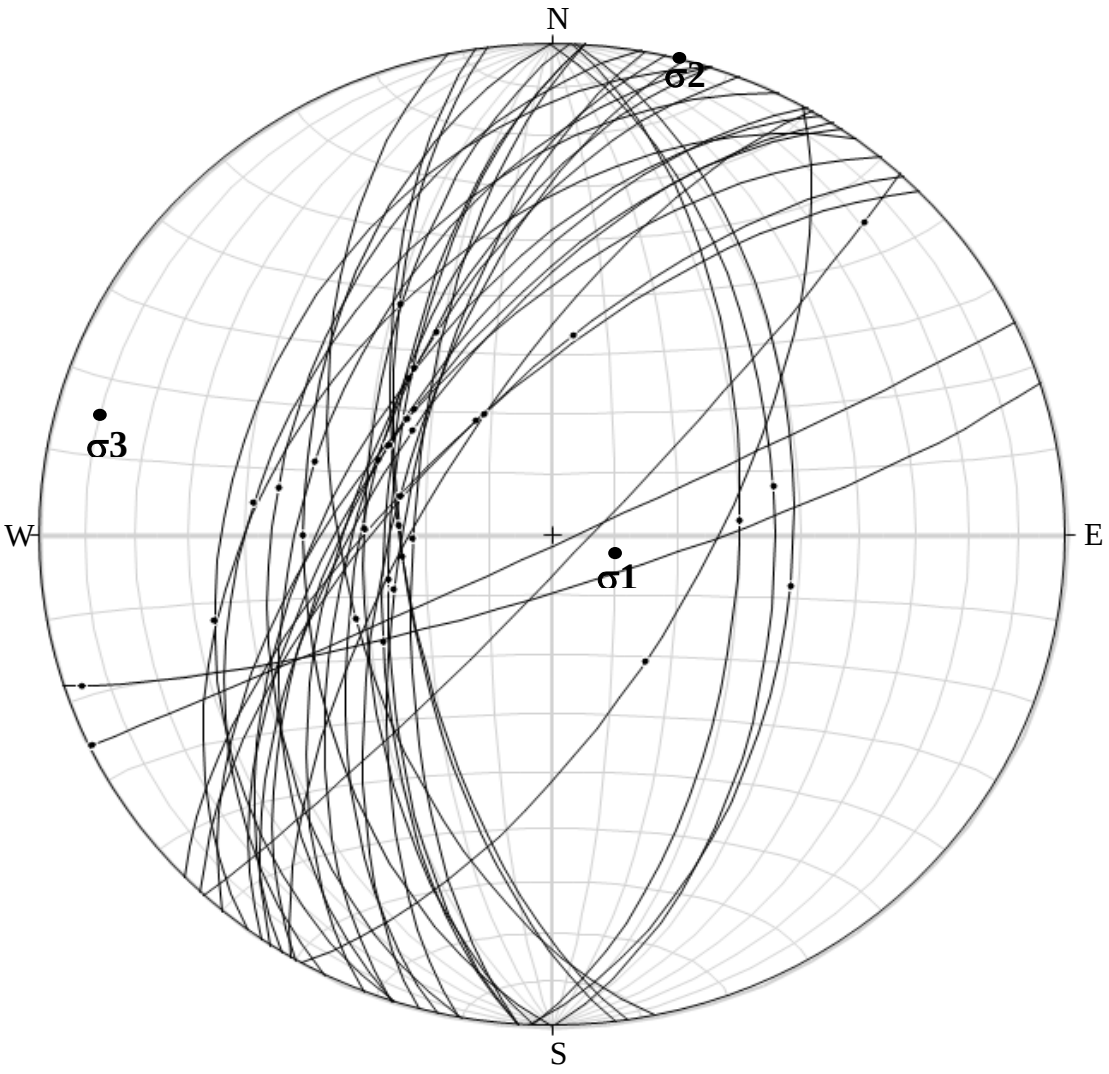

Fig. 5.7 Fault planes and striation with the kinematic axis from kier et al 2006 EAGLE data

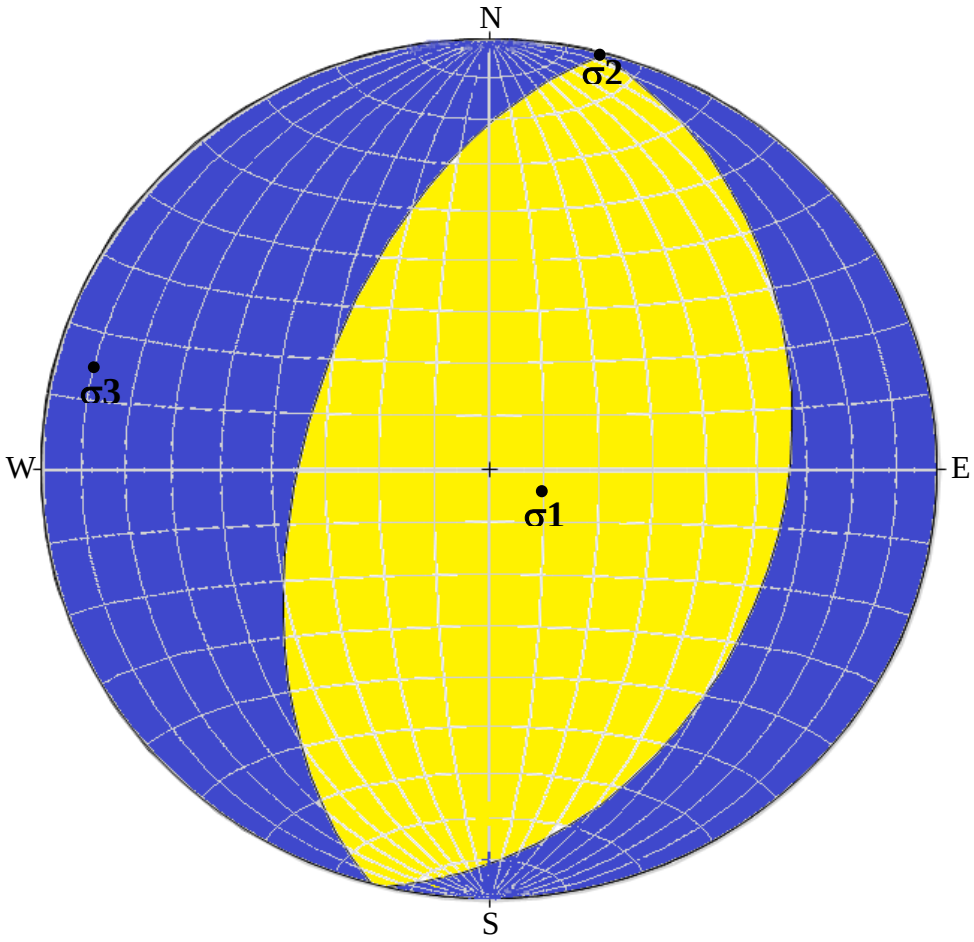

Fig. 5.8 Fault plane solution from Kier et al., 2006; where for σ1: trend= 108, plunge= 79 σ2: trend = 015, plunge= 01 σ3: trend =285, plunge = 11

The above focal mechanism solution for total of 33 fault data indicate predominantly normal dip slip faults that strike approximately north to approximately NNE.

Overall, analysis Agostini et al., 2011 suggests that the difference in the distribution and style of extensional deformation in these rift sectors reflects a difference in rift evolution. Rifting is indeed characterized by a transition from boundary faults and marginal deformation during the initial stages to rift-central magmatic deformation in the latest stages preceding breakup. The characteristics of the central and southern MER accord with a less evolved, purely continental rifting stage with respect to the northern MER, where the tectono -magmatic characteristics point to an incipient breakup stage with Wonji segments acting as incipient oceanic spread ing centers [e.g.,Keranen et al.,2004;Ebinger, 2005;Rooney et al., 2007; Corti, 2009].

From 28 fault slip data collected from the field in relation with inversion of Agostini et al., 2011 and focal mechanism solution resulted from the total of 33 data from kier et al., 2006 it is possible to suggest that the fault system coincides with that of the faulting of the northern main Ethiopian rift which is a normal dip slip fault. Similar to the eastern margin of central main Ethiopian rift most of faults are striking NNE and approximately NE direction.

The inversion data of Agostini et al., 2011 results the minimum compressive stress σ3 is about N90°–110°E extension across the MER , which fits within errors, and Kier et al., 2006; results the minimum compressive stress σ3 is about N103^{o}E orientation within errors of determined extension direction. The result of our present study from the 28 fault slip data results a focal mechanism solution of minimum compressive stress of the extensional direction σ3 is N 120^{o} E with errors. Which is almost similar in extension direction obtained from the inversion of Agostini et al., 2011 and Kier et al., 2006 data. Thus, the inversion of data from Kier et al., 2006 and the focal mechanism of present study results show that the region is characterized by constant kinematics at least during Quaternary.

CHAPTER SIX

6. CONCLUSION AND RECOMMENDATION

6.1 CONCLUSION

The main aim of this thesis was to study and map deformation pattern and type, to map the kinematic indicators associated with earthquake activities, to determine the local and regional extension from kinematic analysis, studying the tectonic evolution of eastern margin of central Main Ethiopian rift to deal with the geometry, kinematics of fault systems. Systematic field observations, satellite imagery analysis, structural mapping of kinematic indicators has been used in order to achieve this aim of study.

Kinematic analysis show that faults are high angle and no evidence for oblique slip movement on the fault planes. Observations also show that extensional features are more remarkable throughout the study area. The results of our analysis show that the roughly NNE to SSW, NE to SW, ENE to WSW and NNW-SSE striking four different fault geometries in the eastern margin. However, to make a detail analysis on the different groups of faults is limited due to few datasets.

The kinematic analysis of slip data from the faults with kinematic indicators measured on the field depicts a stress field characterized by trend and plunge value of minimum horizontal compressive stress direction $\sigma 3 = 120/30$.

The kinematic analysis in the central MER is compared with independent structural investigation (Agostini et al. 2011) and earthquake focal mechanism data (Ayele et al. 2000; Keir et al. 2006). The observed $\sigma 3$ direction from this study is similar to both structural and focal mechanism inversion results showing that the region is characterized by constant kinematics during Quaternary.

6.2 RECOMMENDATION

- Detailed topographic surveys of the trenches have to be conducted, in order to aid geomorphologic markers analysis and fault offset.
- Detailed investigation into Quaternary deformation in eastern margin can be tested by studying of geomorphic features in response to the activity of faults; for a seismo-tectonic study that is helpful to understand recent deformation in eastern margin of central main Ethiopian rift.
- Broad structural and tectonic investigation is required for the analysis of the geometry and kinematics, for spatial and temporal analyses of displaced rock units and geochronology of different parts of the fault system.

REFERENCES

Abebe, Tsegaye, Manetti, P., Bonini, M., Corti, G., Innocenti, F., Mazzarini, F. and Pecskay, Z. (2005). Geological map (scale 1:200000) of the northern main Ethiopian rift and its implication for the volcano-tectonic evolution of the rift, Geological Society of America.

Abebe Tsegaye, Balestrieri, M.L. and Bigazzi, G. (2010). The Central Main Ethiopian Rift is younger than 8 Ma: confirmation through apatite fission-track thermo chronology, *Terra Nova,* **22**: 470–476.

Acocella, V. and Korme, T. (2002). Holocene extension direction along the Main Ethiopian Rift, East Africa. *Terra Nova,* **14**: 191-197.

Acocella, V., Korme, T. and Salvini, F. (2003). Formation of normal faults along the axial zone of the Ethiopian Rift, *Journal of Structural Geology,* **25**: 503–513.

Agostini, A., Bonini, M., Corti, G., Sani, F. and Mazzarini, F. (2011). Fault architecture in the Main Ethiopian Rift and comparison with experimental models: Implications for rift evolution and Nubia–Somalia kinematics, *Earth and Planetary Sci. Lett.* **301**: 479–492.

Almond, D.C. (1986). Geological evolution of the Afro-Arabian dome. *Tectonophysics*, **131**: 301–332.

Argus, D.F. and Gordon, R.G. (1991). No-net-rotation model of current plate velocities incorporating plate motion model. *Geophys. Res. Lett.* **18**: 2039–2042.

Atalay Ayele (2000) Normal left-oblique fault mechanism as an indication of sinistral deformation the Nubia and Somalia plates in the main Ethiopian rift. *African Earth Sciences,* 31: 359-367.

Bastow, I.D., Stuart, G.W., Kendall, J.M. and Ebinger, C.J. (2005). Upper mantle seismic structure in a region of incipient continental breakup: Northern Ethiopian rift, *Int.* Geophys. **162**: 479–493.

Bastow, I.D., Pilidou, S., Kendall, J-M. and Stuart, G.W. (2010). Melt- induced seismic anisotropy and magma assisted rifting in Ethiopia: Evidence from surface waves, *Geochem. Geophys. Geosyst.* **11**: 1-19.

Bekele Abebe, (1993). Studio geologico-structurale Del Rift Etiopico a sud di Assela. Ph. D Dissertation. University of Firenze, Firenze, Italy, 153 pp.

Bendick, R., Bilham, R., Asfaw, L. and Klemperer S. (2006). Distributed Nubia-Somalia relative motion and dyke intrusion in the Main Ethiopian Rift, *Geophys. J. Int.* **165**: 303–310.

Benoit, M.H., Nyblade, A.A. and VanDecar, J.C. (2006). Upper mantle P-wave speed variations beneath Ethiopia and the origin of the Afar hotspot, *Geology*, **34**: 329–332.

Benvenuti, M., Carnicelli, S., Belluomini, G., Dainellia, N., Di Grazia, S., Ferrari, G.A., Iasio, C., Sagri, M., Ventra, D., Balemwal Atnafu and Seifu Kebede (2002). The Ziway–Shala lake basin (main Ethiopian rift, Ethiopia): a revision of basin evolution with special reference to the Late Quaternary, *African Earth Sci.* **35**: 247–269.

Benvenuti, M., Bonini, M., Tassi, F., Corti, G., Sani, F., Agostini, A., Manetti, P. and Vaselli, O. (2013). Holocene lacustrine fluctuations and deep CO2degassing in the northeastern Lake Langano Basin (Main Ethiopian Rift), *African Earth Sci.* **77**: 1-10.

Berhe, S.M.., 1978. Geological map (1:250,000) sheet NC37-15 (Nazret). Geological Survey of Ethiopia.

Bigazzi, B., Bonadonna, F., Di Paola, G. and Giuliani, A. (1993). K-Ar and fission tracks ages of the last volcano-tectonic phases in the Ethiopian Rift Valley (Tulu Moye area), *Geology and mineral resources of Somalia and Surrounding Regions*, **113**: 311-322.

Bilham, R., Bendick, R., Larson, K., Mohr, P., Braun, J., Tesfaye, S. and Asfaw L. (1999). Secular and tidal strain across the Main Ethiopian Rift, *Geophys. Res. Lett.*, **26**: 2789 –2792.

Boccaletti, M., Getaneh, A. and Tortorici, L. (1992). The Main Ethiopian Rift: an example of oblique rifting, *Ann. Tecton.* **6**: 20–25.

Boccaletti, M., Bonini, M., Mazzuoli, R., Abebe Bekele, Piccardi, L. and Tortorici, L. (1998). Quaternary oblique extensional tectonics in the Ethiopian Rift (Horn of Africa), *Tectonophysics*, **287**: 97–116.

Boccaletti, M., Bonini, M., Mazzuoli, R. and Trua, T. (1999). Pliocene-Quaternary volcanism and faulting in the northern Main Ethiopian Rift (with two geological maps at scale 1:50,000), *Acta Vulcanologica,* **11**: 83–97.

Bonini, M., Souriot, T., Boccaletti, M. and Brun, J.P. (1997). Successive orthogonal and oblique extension episodes in a rift zone: laboratory experiments with application to the Ethiopian Rift, *Tectonics*, **16**: 347–362.

Bonini, M., Corti, G., Innocenti, F., Manetti, P., Mazzarini, F., Abebe Tsegaye and Pecskay, Z. (2005). Evolution of the Main Ethiopian Rift in the frame of Afar and Kenya rifts propagation, *Tectonics **24**:* 1-25.

Casey, M., Ebinger, C. J., Keir, D., Gloaguen, R. and Mohamad, F. (2006). Strain accommodation in transitional rifts: Extension by magma intrusion and faulting in Ethiopian rift magmatic segments, in The Afar Volcanic Province With in the East African Rift System, *Geol. Soc. Spec. Publ,* **259**: 143–163.

Chernet, T., Hart, W.K., Aronson, J.L. and Walter, R.C. (1998). New age constraints on the timing of volcanism and tectonism in the northern Main Ethiopian Rift-southern Afar transition zone (Ethiopia), *Volcanology and Geothermal Research,* **80**: 267–280.

Chorowicz, J., Collet, B., Bonavia, F. and Tesfaye Korme (1994). Northwest to north-northwest extension direction in the Ethiopian Rift deduced from the orientation of extension structures and fault slip analysis, *Geological Society of American Bulletin,* **105**:1560 – 1570.

Chu, D. and Gordon, R.G. (1999). Evidence for motion between Nubia and Somalia along the Southwest Indian Ridge. *Nature,* **398**: 64-67.

Corti, G. (2008). Control of rift obliquity on the evolution and segmentation of the main Ethiopian rift. *Nature Geoscience,* **1**: 258–262.

Corti, G. (2009). Continental rift evolution: From rift initiation to incipient break-up in the Main Ethiopian Rift, East Africa. *Earth-Sci. Review,* **96**: 1–53.

Collet, B., Taud, H., Parrot, J. F., Bonavia, F. and Chorowicz, J. (2000). A new kinematic approach for the Danakil block using a Digital Elevation Model representation, *Tectonophysics*, **316**: 343– 357.

Dagnachew Legesse, Vallet-Coulomb, C. & Gasse, F. (2004). Analysis of the hydrological response of a tropical terminal lake, Lake Abiyata (Main Ethiopian Rift Valley) to changes in climate and human activities, *Hydrological Process,* **18**: 487-504.

Davidson, A. and Rex, D.C. (1980). Age of volcanism and rifting in south-western Ethiopia. *Nature,* **283**: 654–658.

Di Poala, G.M. (1972). The Ethiopian Rift Valley (between 7º00' and 8º40' Lat. North). *Bulletin of Volcanology,* **35**: 497-506.

Di Paola, G.M. (1976).Geological Map of the Tullu Moye` Volcanic Area (Arusi: Ethiopian Rift valley). 1: 75,000 Scale. Laboratorio di Geocronologia e Geochimica isotopica, CNR, Pisa, Italy.

Di Pola, G.M. (1977). Geological map of Tulu Moye volcanic area. Scale (1:75,000).

Di Paola, G.M., Seife, M.B. and Arno, V. (1993). The Kella horst: its origin and significance in crustal attenuation and magmatic processes in the Ethiopian Rift Valley. In: Geology and Mineral Resources of Somalia and Surrounding Regions*, Ist. Agronom. Oltremare, Firenze, Relaz. Monograf,* **113**: 323–338.

Ebinger, C.J., Bechtel, T.D., Forsyth, D.W. and Bowin, C.O. (1989). Effective elastic plate thickness beneath the East African and Afar plateaus and dynamic compensation of the uplifts, *Journal of Geophysical Research,* **94**: 2883– 2901.

Ebinger, C. J., Yemane, T., WoldeGabriel, Giday, Aronson, J. L. and Walter R. C. (1993). Late Eocene-Recent volcanism and faulting in the southern main Ethiopian rift, *Geol. Soc. London,* **150**: 99–108.

Ebinger, C.J., Yemane, T., Harding, D.J., Tesfaye, S., Kelley, S. and Rex, D.C. (2000). Rift deflection, migration, and propagation: linkage of the Ethiopian and Eastern rifts, Africa, *Geological Society of America Bulletin,* **112**: 163–176.

Ebinger, C.J. and Casey, M. (2001). Continental breakup in magmatic provinces: An Ethiopian example. *Geology Society of America Bulletin*, **12**: 527–530.

Ebinger, C. (2005). Continental break-up: The East African perspective. *Astron. Geophys.* **46**: 2.16–2.21.

Fernandes, R., Ambrosius, B., Noomen, R., Bastos, L., Combrink, L., Miranda, J. and Spakman, W. (2004). Angular velocities of Nubia and Somalia from continuous GPS data: Implications on present-day relative kinematics, *Earth planet.sci.lett.* **222**: 197-208.

George, R. and N. Rogers (2002). Plume dynamics beneath the African plate inferred from the geo-chemistry of the Tertiary basalts of southern Ethiopia. *Contrib. Mineral. Petrol.* **144**: 286–304.

Gianelli, G. and Teklemariam, M. (1993). Water – rock intraction processes in the Aluto- Langano geothermal field. *Journal of Volcanology and Geothermal Resource*, **56**: 429 – 445.

Gibson, I.L. (1969). The structure and volcanic geology of an axial portion of the Main Ethiopian Rift. *Tectonophysics*, **8**: 561-565.

Gouin, P. (1979). *Earthquake History of Ethiopia and the Horn of Africa.* Int. Dev. Res. Cent.Ottawa, Ont. Canada, 258 pp.

Hayward, N.J. and Ebinger, C.J. (1996). Variation in the long –axis segmentation of the afar rift system. *Tectonics,* **15**: 244-257.

Hofmann, C., Courtillot, V., Feraud, G., Rochette, P., Yirgu, G., Ketefo, E. and Pik, R. (1997). Timing of the Ethiopian flood basalts event and implications for plume birth and global change, *Nature,* **389**: 838–841.

Jestin, F., Huchon, P. and M. Gaulier, M. (1994). The Somalia plate and the East African Rift system: Present-day kinematics, *Geophys. J. Int.* **116**: 637–654.

Kazmin, V. (1972). Geological map of Ethiopia. Scale (1:2000, 000). Geological survey of Ethiopia, Ministry of Mines, Addis Ababa.

Kazmin, V. and Berhe, S.M. (1978). Geology and development of the Nazret area, northern Ethiopian Rift: *Sheet NC37-15,* 3: 26.

Kazmin, V. (1979). Stratigraphy and correlation of volcanic rocks in Ethiopia. *Ethiopian Institute of Geological surveys,* **106**: 1-26.

Kazimin, V. (1980). Transform faults in the East African Rift System. *Atti Conv. Lincei,* **47**: 65-73.

Kazmin, V. and Seife, M.B. (1978). Geology and development of the Nazreth area, Northern Ethiopia Rift. *Geol. Surv. of Ethiopia.*

Keir, D., Ebinger, C. J., Stuart, G. W., Daly, E. & Ayele, A. (2006). Strain accommodation by magmatism and faulting as rifting proceeds to breakup: Seismicity of the northern Ethiopian rift, *Geophys. Res.* **111**: 1-17.

Keir, D., Bastow, I.D., Whaler, K.A., Daly, E., Cornwell, D.G. and Hautot, S. (2009). Lower crustal earthquakes near the Ethiopian rift induced by magmatic processes. *Geochem. Geophys. Geosyst.* **10**: 1–10.

Kendall, J.M., Stuart, G.W., Ebinger, C.J., Bastow, I.D. and Keir, D. (2005). Magma assisted rifting in Ethiopia, *Nature,* **433**: 146–148.

Keranen, K., Klemperer, S.L., Gloaguen, R. and EAGLE Working Group (2004).Three-dimensional seismic imaging of a protoridge axis in the Main Ethiopian Rift, *Geology,* **32**: 949–952.

Korme, T., Chorowicz, J., Collet, B. and Bonavia, F.F. (1997). Volcanic vents rooted on extension fractures and their geodynamic implications in the Ethiopian Rift, *Volcanol. Geotherm. Res.* **79**: 205-222.

Kurz, T., Gloaguen, R., Ebinger, C., Casey, M. and Abebe, B. (2007). Deformation distribution and type in the Main Ethiopian Rift (MER): a remote sensing study, *African Earth Sciences,* **48**: 100–114.

Le Pichon, X. and Gaulier, J.M. (1988).The rotation of Arabia and the Levant fault system. *Tectonophysics,* **153**: 271–294.

Le Turdu, C., Tiercelin, J-J., Gibert, E., Travi, Y., Lezzar, K-E., Richert, J-P., Massault, M., Gasse, F., Bonnefille, R., Decobert, M., Gensous, B., Jeudy, V., Endale Tamrat, Mohammed

Umer Mohammed, Martens, K., Balemwal Atnafu, Tesfaye Chernet, Williamson, D. and Taieb, M. (1999). The Ziway–Shala lake basin system, Main Ethiopian Rift: Influence of volcanism, tectonics, and climatic forcing on basin formation and sedimentation, *Palaeogeography, Palaeoclimatology, Palaeoecology* **150:** 135–17.

Levitte, D., Columba, J. and Mohr, P. (1974). Reconnaissance geology of the Amaro Horst, southern Ethiopian Rift, *Geological society American Bulletin,* **85**: 417-422.

Merla, G., Abbate, E., Azzaroli, A., Bruni, P., Canuti, P., Fazzuali, M., Sagri, M. and Tacconi, P. (1979). A geological map of Ethiopia and Somalia, and comment, CNR, Firenze.

Meyer, W., Pilger, A., Rosler, A.and Slets, J. (1975).Tectonic evolution of the northern part of the Main Ethiopian Rift in southern Ethiopia. Pp. 352-362.

Mohr, P. (1962). The Ethiopian Rift system. *Bull. Geol. Obs.* **5**:33-62.

Mohr, P. (1967). Major volcano-tectonic lineament in the Ethiopian Rift System. *Nature,* **213**: 664-665.

Mohr, P. (1970). The Geology of Ethiopia. Addis Ababa University Press. Addis Ababa. Pp. 1-268.

Mohr, P. (1983). Ethiopian flood basalt province. *Nature*, **303**: 577 – 584.

Mohr, P. (1987). Pattern of faulting in the Ethiopian Rift Valley. *Tectonophysics,* **143**:169 -179.

Mohr, P. and Wood, C.A. (1976). Volcano spacing and lithospheric attenuation in the Eastern Rift of Africa, Earth Planet. *sci.lett.* **33**:126-144.

Mohr, P.A., Mitchell, J.C. and Raynolds, R.G.H. (1980). Quaternary volcanism and faulting at O'A Caldera, Central Ethiopian Rift. *Bulletin of Volcanology,* **43**: 173–189.

Mohr, P. and Zanettin, B. (1988). The Ethiopian food basalt province. In: Continental flood basalts, Kluwer Academic Publishers, Dordrecht. Pp. 63–110.

Pik, R., Deniel, C., Coulon, C., Yirgu, G., Hofmann, C. and Ayalew, T. (1998). The northwestern Ethiopian Plateau flood basalts: classification and spatial distribution of magma types. *Volc. Geoth. Res.* **81**: 91–111.

Pizzi, A., Coltorti, M., Abebe Bekele, Disperati, L., Sacchi, G. and Salvini, R. (2006). The Wonji Fault Belt (Main Ethiopian Rift, Ethiopia): Structural and geomorphological constraints and GPS monitoring, in The Afar Volcanic Province with in the East African Rift System, Geological society, London, Special Pub. **259**: 191 – 207.

Rooney, T., Furman, T., Bastow, I., Ayalew, D. and G. Yirgu (2007). Lithospheric modification during crustal extension in the Main Ethiopian Rift, *Geophys. Res.* **112**:1-21.

Sagri, M. and the staff of EU Project, (1998). Land resources inventory, environmental change analysis and their application to agriculture in the Lakes Region (Ethiopia) Final report. European Commission.

Seth, B., Gloaguen, R., Thirlwall, M., Pfaender, J., Yirgu, G. and Wnorowska, U. (2005). Quaternary fissural basalts in the Main Ethiopian Rift, EGU Conference, Vienna, April 2005.

Street, F.A. (1979). Late Quaternary lakes in the Ziway–Shala Basin, Southern Ethiopia. Unpublished Ph.D. Thesis, University of Cambridge, 475 pp.

Tenalem Ayenew (2004). Environmental implications of changes in the levels of lakes in the Ethiopian Rift since 1970. *Regional environmental change*, **4**: 12-204.

Ukstins, I.A., Renne, P.R., Wolfenden, E., Baker, J., Ayalew, D. and Menzies, M. (2002). Matching conjugate volcanic rifted margins: ^{40} Ar/^{39} Ar chronostratigraphy of pre- and syn-rift bimodal flood volcanism in Ethiopia and Yemen. *Earth Planet. Sci. Lett.* **198**, 289–306.

UNDP (1973). Geology, geochemistry and hydrogeology of hot springs of the East African Rift System within Ethiopia. New York.

WoldeGabriel, Giday, and Aronson, J. (1987). The Chow Bahir Rift: a"failed" rift in Southern Ethiopia. *Geology*, **15**: 430–433.

WoldeGabriel Giday, Aronson, J.L. and Walter, R.C. (1990). Geology, geochronology and rift basin development in the central sector of the Main Ethiopian Rift, *Bull. Geol. Soc. Am.* **102**: 439–458.

WoldeGabriel, Giday, Yemane, T., White, T., Asfaw, B. and Suwa, G. (1991). Age of volcanism and fossils in the Burji-Soyoma area, Amaro Horst, southern Main Ethiopian Rift, *Afr. Earth Sci.* **13**: 437– 447.

WoldeGabriel Giday (2002). The Main Ethiopian Rift System: an overview on volcanic, tectonic, rifting, and sedimentation processes, In Ethiopian Rift Valley lakes (ed. C. Tudorancea and W.D. Taylor. Backhuys Publishers, Leiden) pp 13-43.

Wolfenden, E., Ebinger, C., Yirgu, G., Deino, A. and Ayele, D. (2004). Evolution of the northern Main Ethiopian Rift: Birth of a triple junction, *Earth Planet. Sci. Lett.* **224**: 213–228.

Zanettin, B., Justin, B., Nicoletti, M. and Petrucciani, C. (1978). The evolution of the Chencha escarpment and the Ganuji graben (Lake Abaya) in the southern Ethiopian Rift. *Geological Bulletin,* **8**: 473-490.